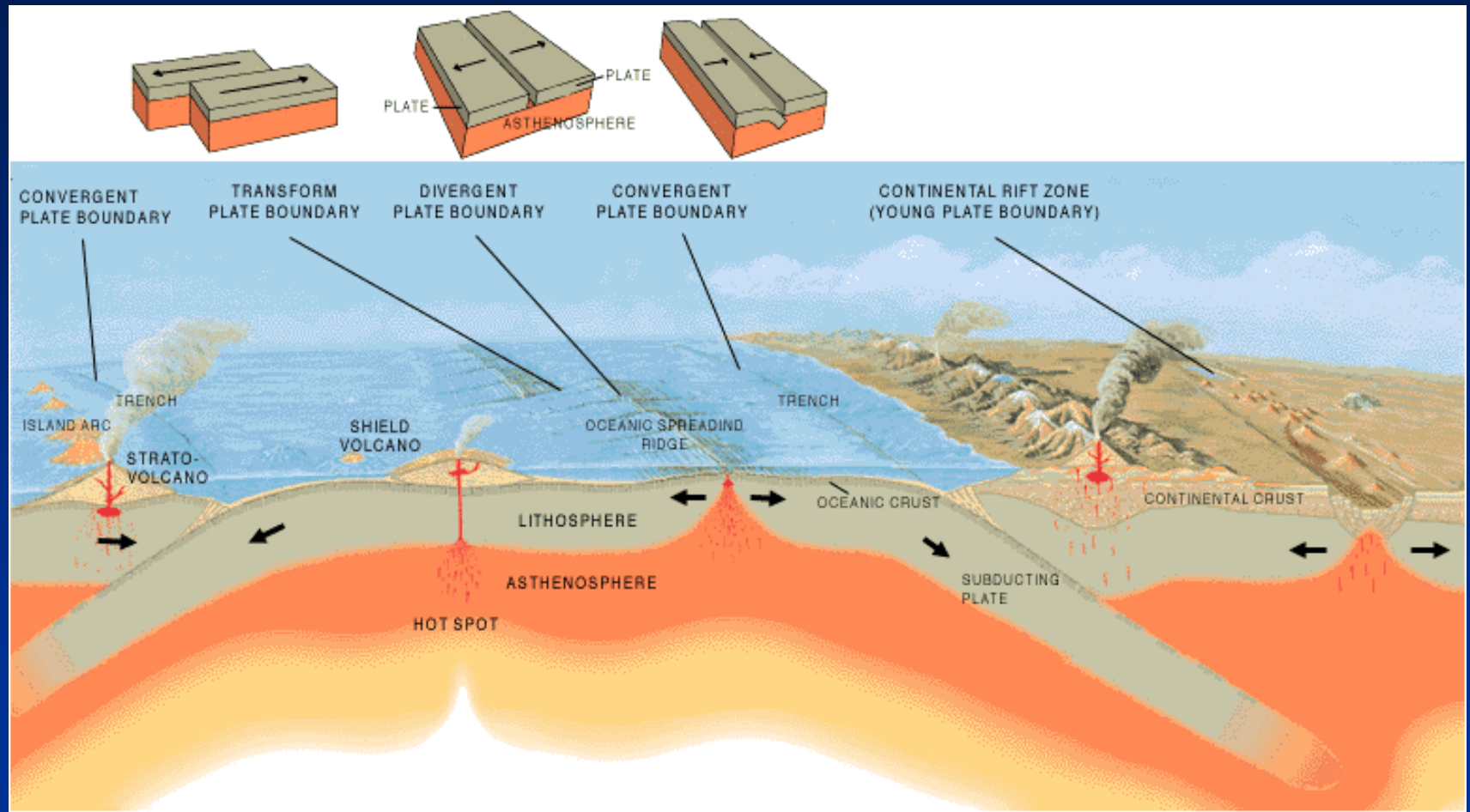


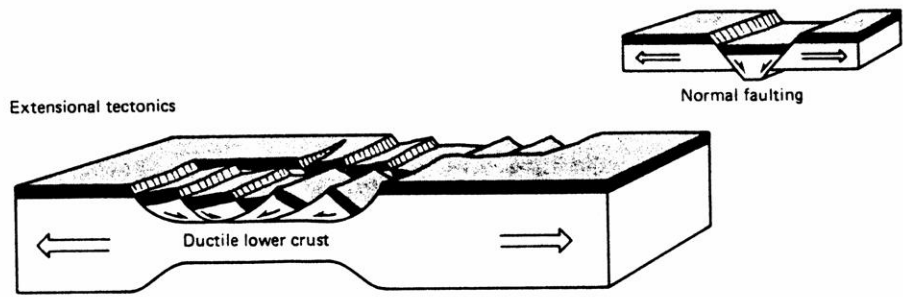
Tettonica a zolle, il sistema e i tipi di margini di placche



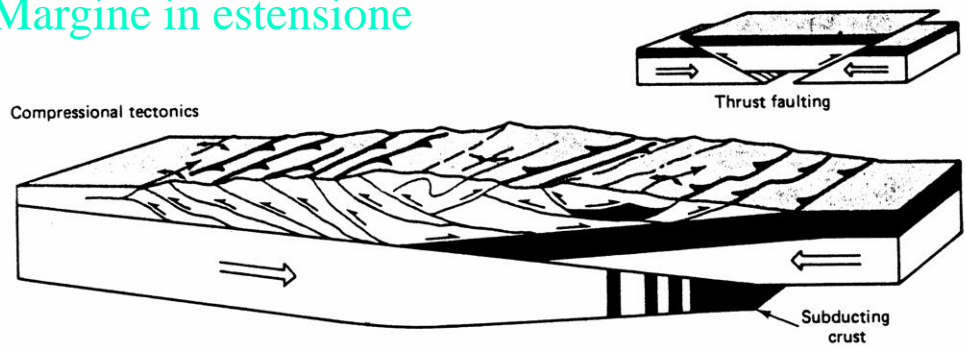
Da "The dynamic Earth" in USGS Web Site

Immagini e fotografie tratte da:

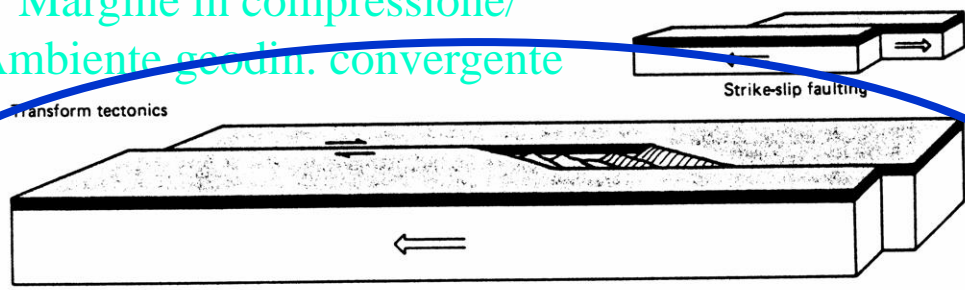
- Bohrmann et al., 2003. *Geo-Marine Letters*, 23, 239–249
- Brown K.M., Orange D.L., 1993. Structural aspects of diapiric m61ange emplacement: the Duck Creek Diapir. *Journal of Structural Geology*, 15, 831-847.
- Debelmas J., Mascle G., Basile C., 2008. *Les Grandes Structures Géologiques*, 5^e edition. Dunod.
- Deville E., 2009. Mud Volcano Systems. In: *Volcanoes: Formation, Eruptions and Modelling* Editors: N. Lewis, A. Moretti, Nova Science Publishers Inc., 95-126.
- Deville E., Guerlais S-H., Callec Y., Lallemand S, Noble M. and the CARAMBA research team, 2006. Fluid vs Solid Subsurface Sediment Mobilization Processes: Insight from the South of the Barbados Accretionary Prism: *Tectonophysics*, 428, 33-47.
- Fossen H., 2010. *Structural Geology*. Cambridge University Press.
- Gomez F. et al., 2007. Strain partitioning of active transpression within the Lebanese restraining bend of the Dead Sea Fault (Lebanon and SW Syria). *Geological Society, London, Special Publications*, 290, 285-303.
- Hatcher R.D., 1995. *Structural Geology: Principles Concepts and Problems*. Prentice Hall International.
- Hadad A. et al., 2020. Tectonics of the Dead Sea Fault Driving the July 2018 Seismic Swarm in the Sea of Galilee (Lake Kinneret), Israel. *Journal of Geophysical Research: Solid Earth*, 10.1029/2019JB018963.
- Kearey P., Klepeis K.A., Vine F.J., 2009. *Global tectonics*. – 3rd ed. Wiley-Blackwell.
- Kopf A., 2002. Significance of mud volcanism. *Reviews of Geophysics*, 40 (2), 1-52.
- Krastel et al., 2003. *Geo-Marine Letters*, 23, 230–238.
- Mercier J., Vergely P., 1996. *Tettonica*. Pitagora Editore.
- Planke S. et al., 2003. Mud and fluid migration in active mud volcanoes in Azerbaijan. *Geo-Marine Letters*, 23, 258-268.
- Price N.J., Cosgrove J.W., 1990. *Analysis of Geological Structures*. Cambridge University Press.
- Ramsay J. G., Huber M. I., 1987. *The Techniques of Modern Structural Geology. Volume 2: Folds and Fractures*. Academic Press Inc.
- Sumner & Westbrook, 2001. *Marine and Petroleum Geology*, 18, 591-613.
- Suppe J., 1985. *Principles of Structural Geology*. Prentice-Hall Inc.
- van der Pluijm B., Marshak S., 2004. *Earth Structure: An Introduction to Structural Geology and Tectonics*, Second Edition. WW Norton & Company.



Margine in estensione

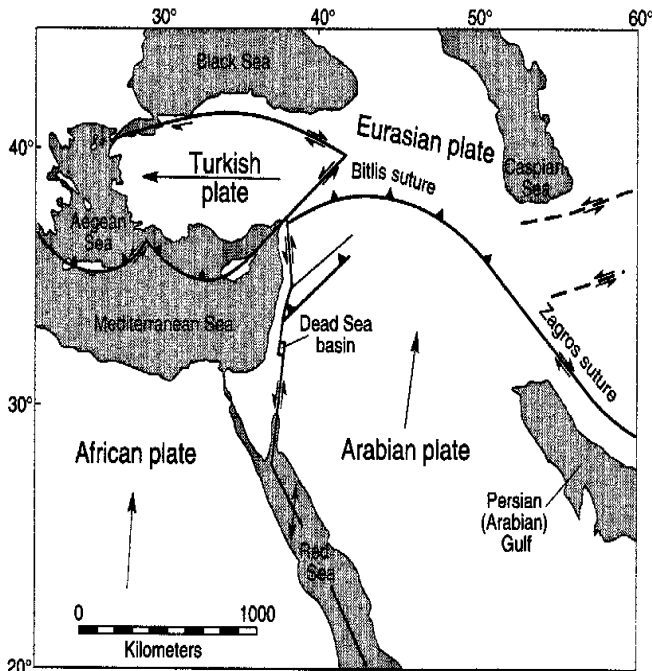


Margine in compressione/
Ambiente geodin. convergente



Margine trasforme/trascorrente

Tipo di margini di
placca e ambienti
geodinamici



Da Hatcher, 1995

Margini in trascorrenza

Ambienti geodinamici in trascorrenza;

tettonica di trascorrenza e trasforme

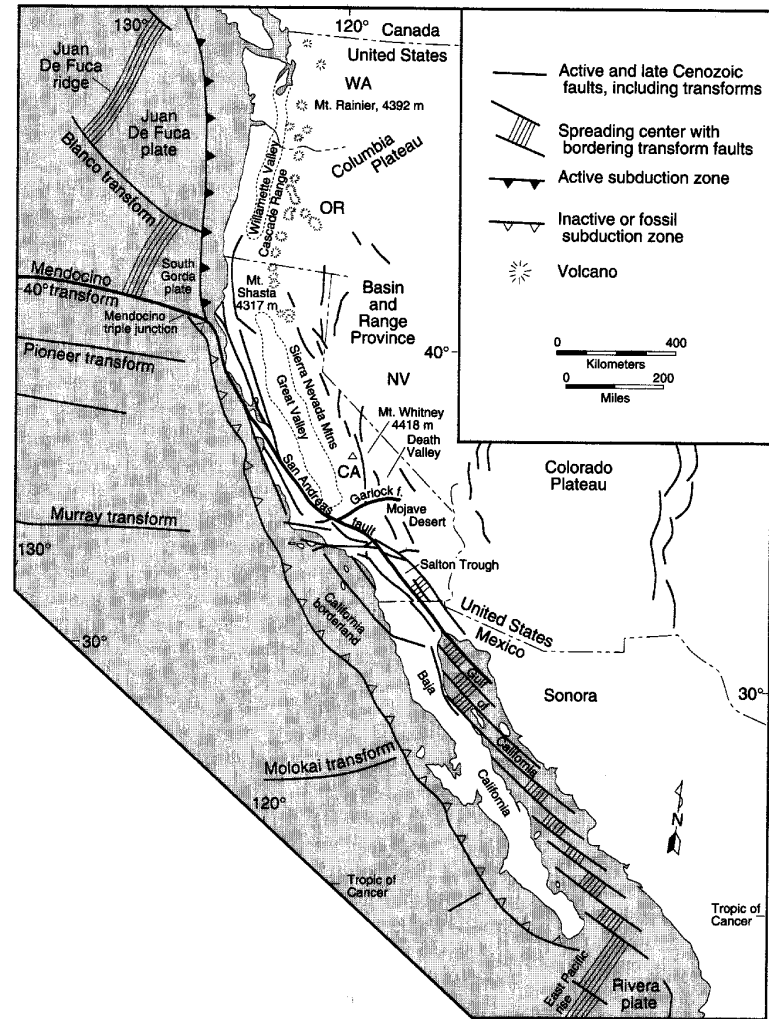


FIGURE 12-12

San Andreas and related fault systems in California, northern Mexico, and in the adjacent Pacific Ocean. (After J. C. Crowell, 1987, *Episodes*, v. 110.)

Da Hatcher, 1995



Da Earth from Space, NASA (eol.jsc.nasa.gov)

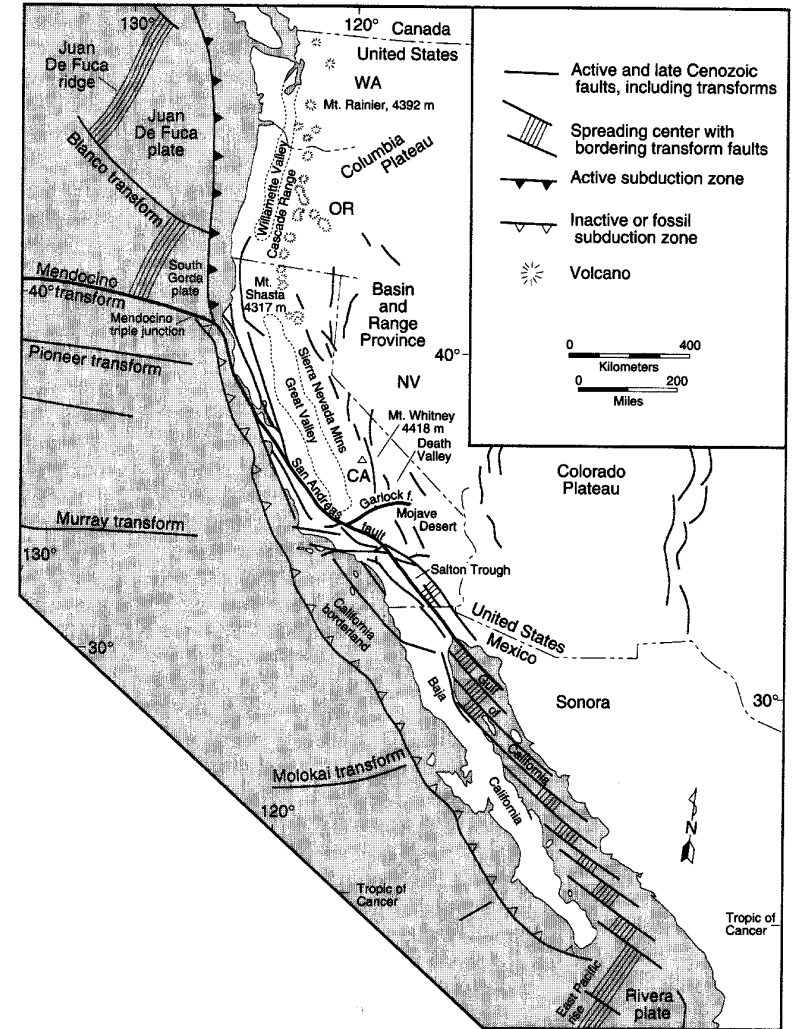
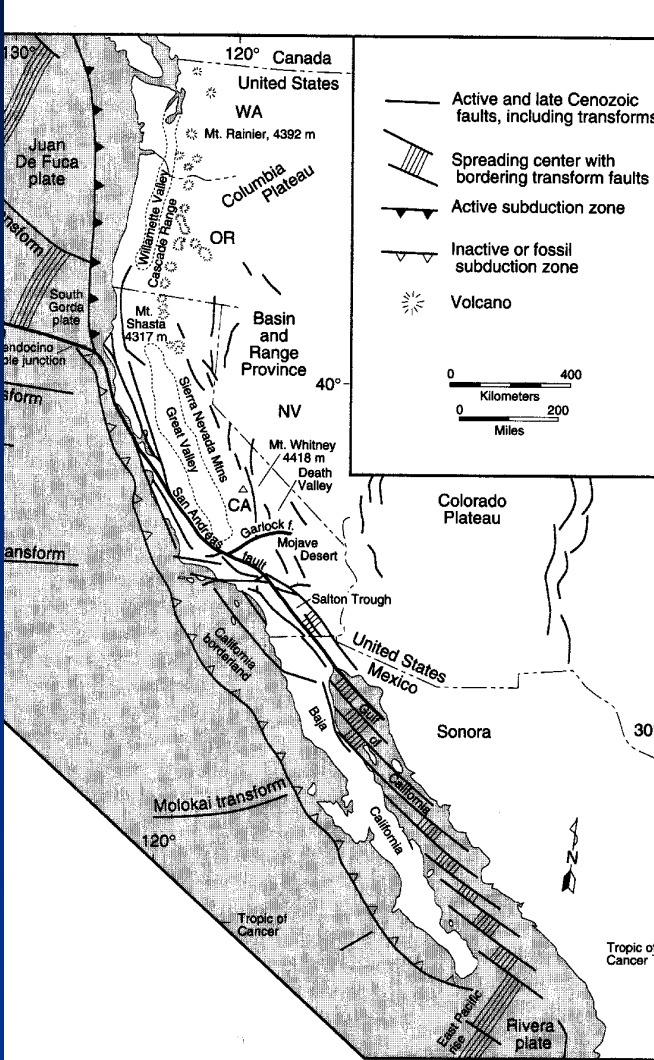
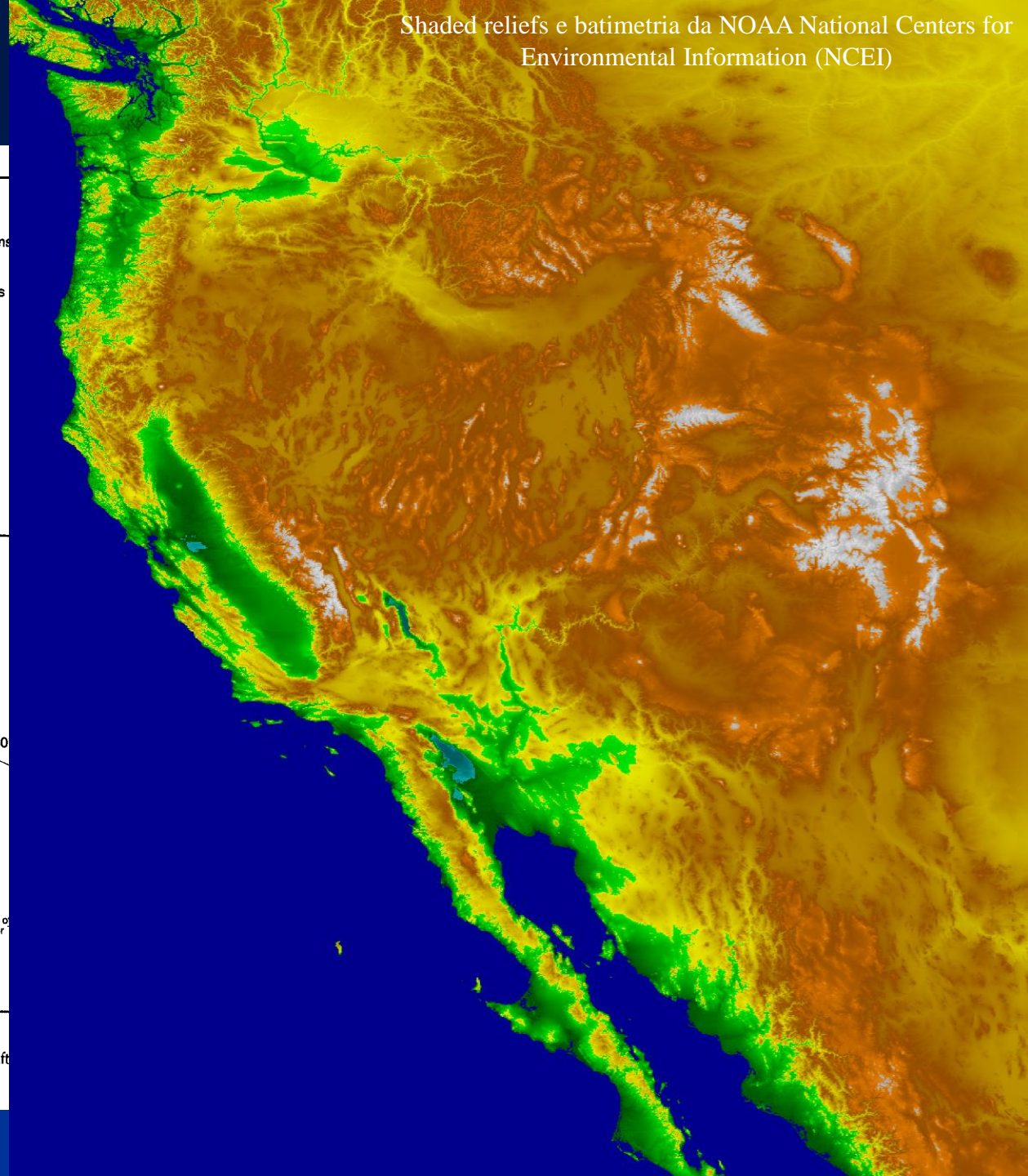


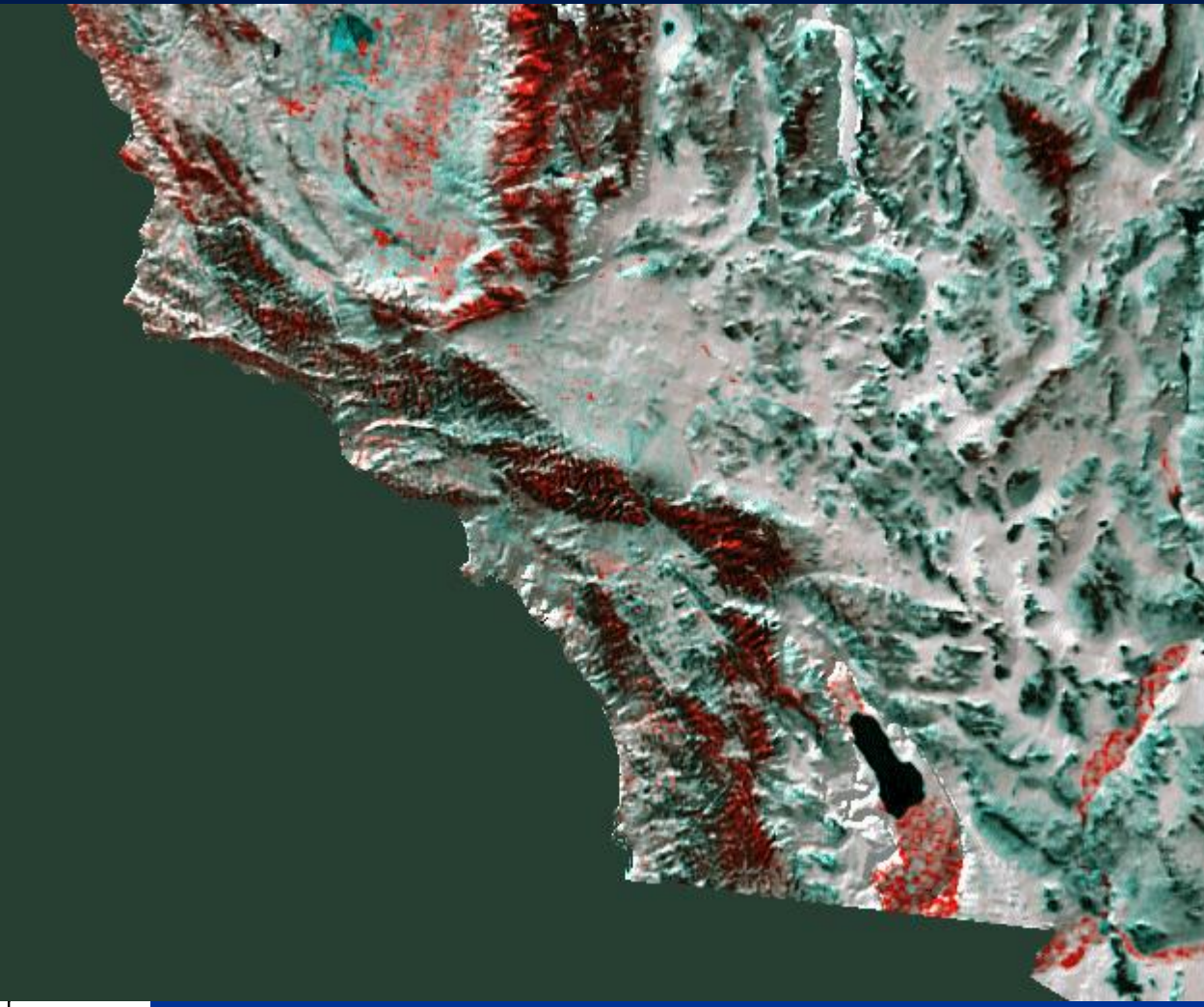
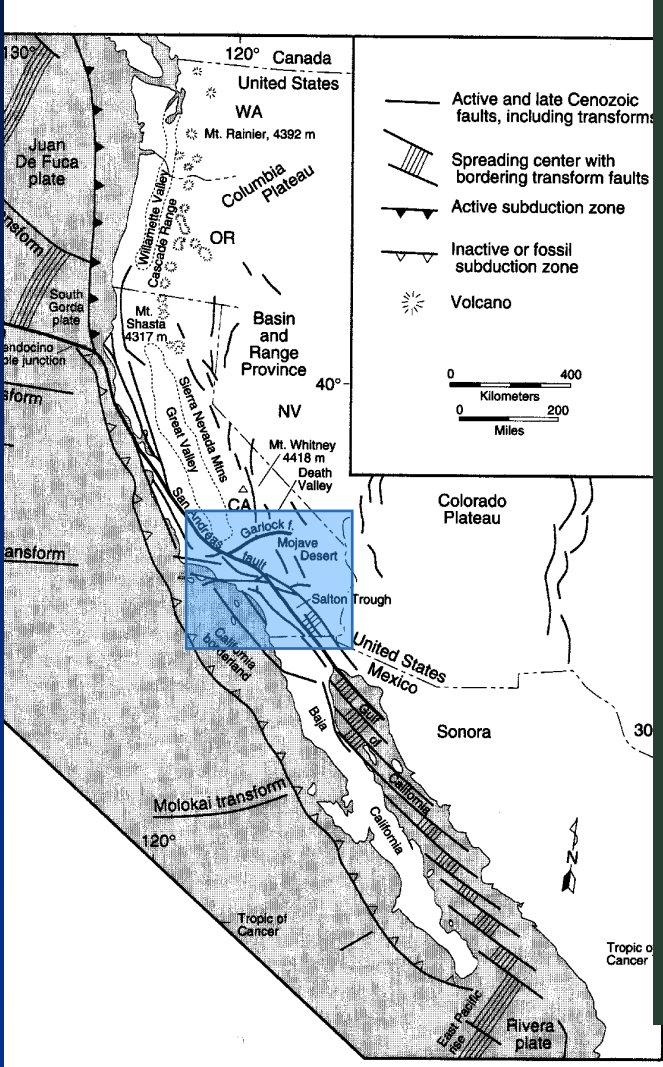
FIGURE 12-12
 San Andreas and related fault systems in California, northern Mexico, and in the adjacent Pacific Ocean. (After J. C. 1987, *Episodes*, v. 110.)

Da Hatcher, 1995



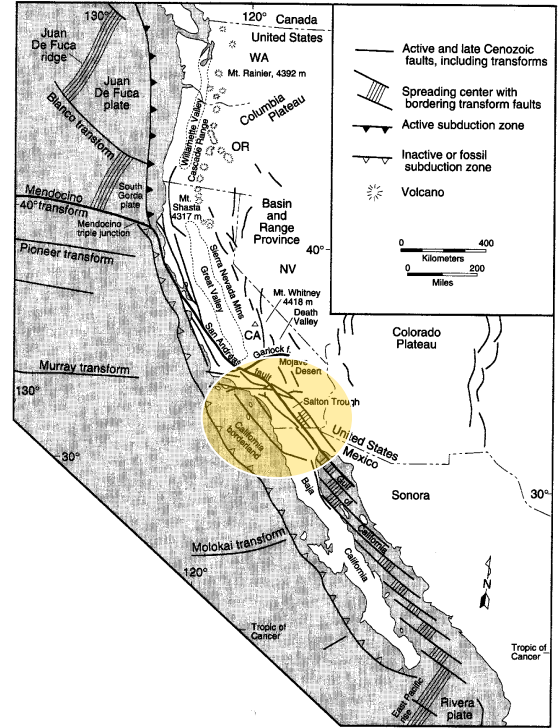
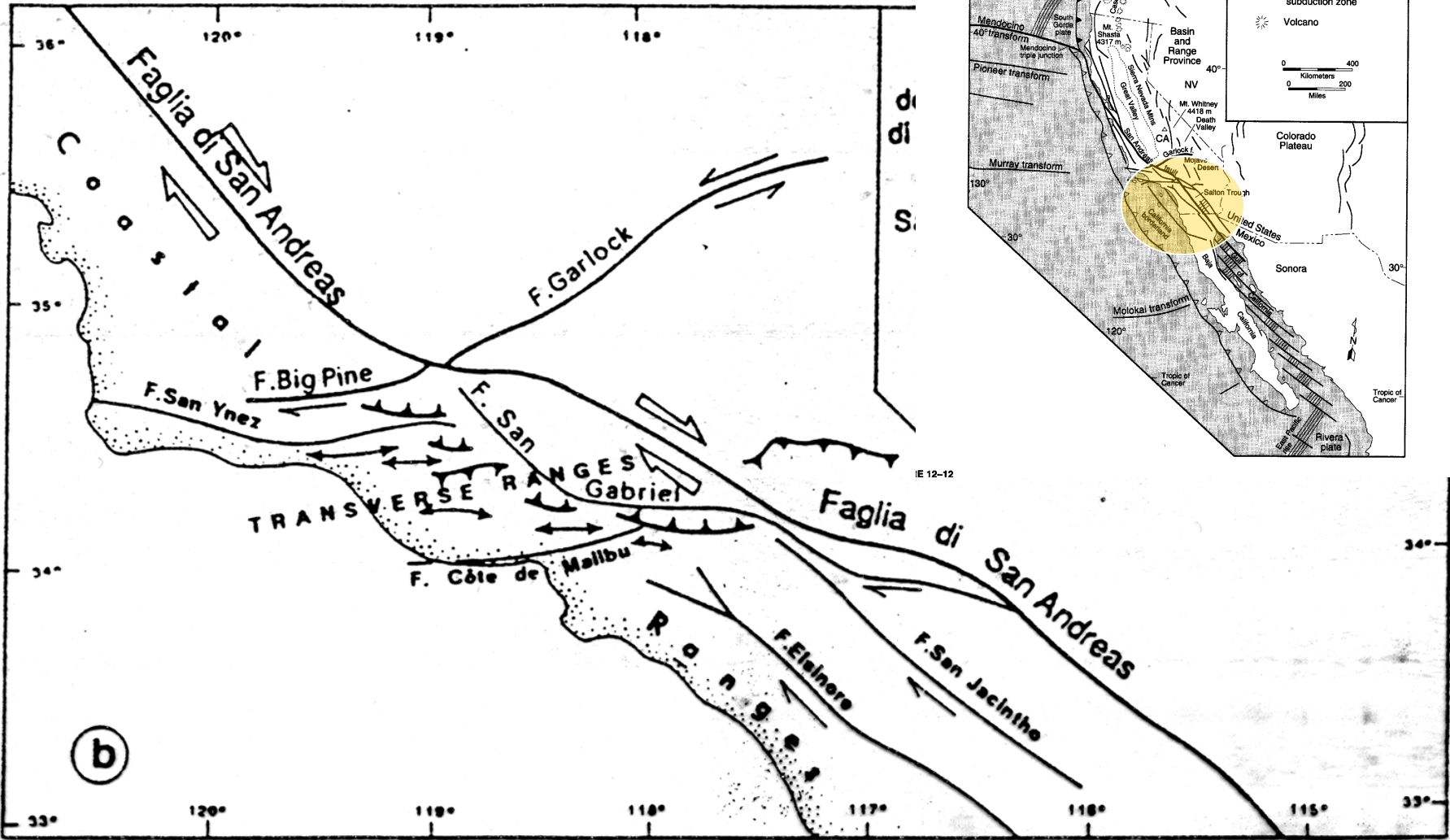
systems in California, northern Mexico, and in the adjacent Pacific Ocean. (Aft





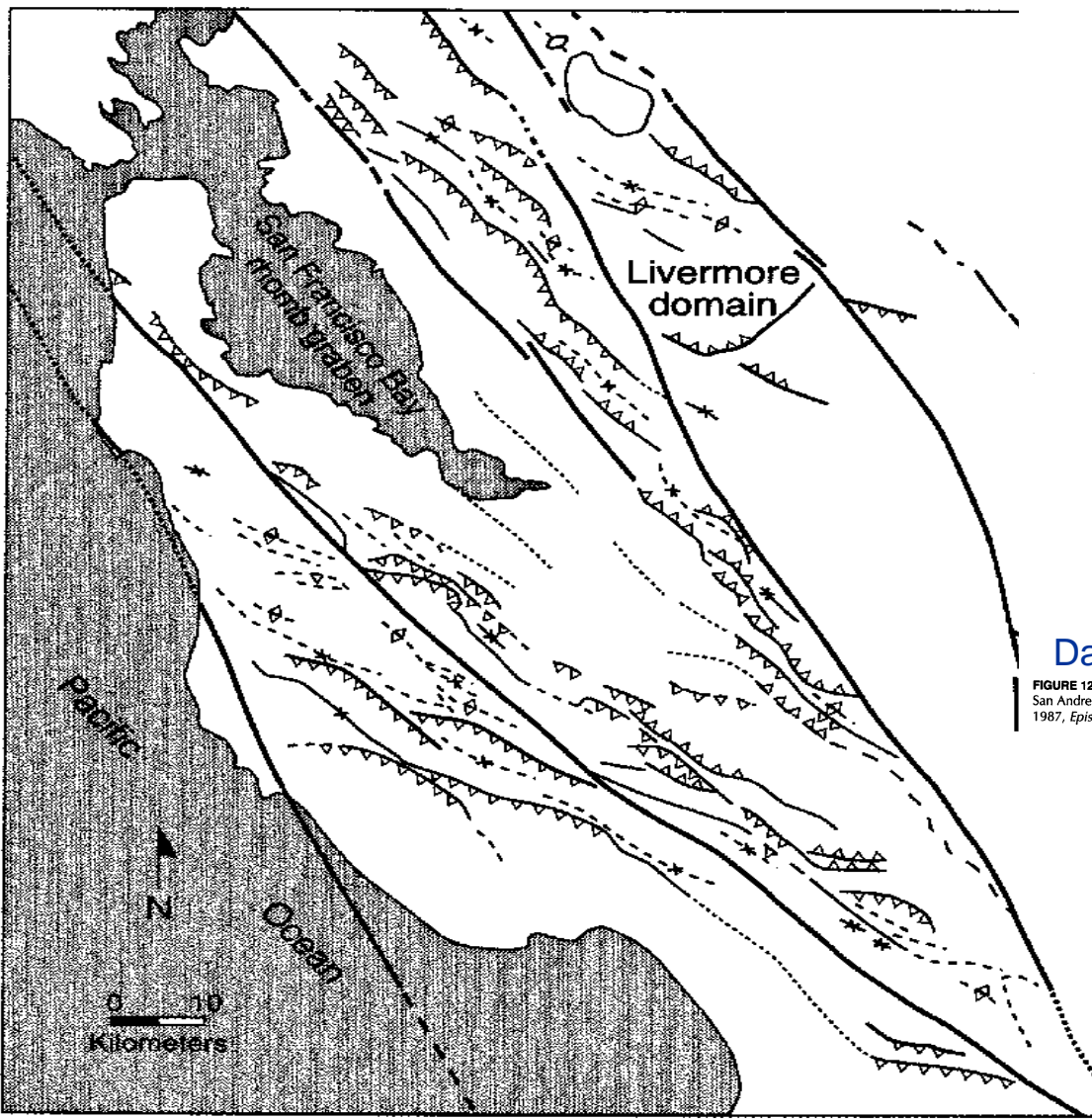
systems in California, northern Mexico, and in the adjacent Pacific Ocean. (After J. C. Crowell,

Da USGS
Mosaico dati satellitari AVHRR, falsi colori

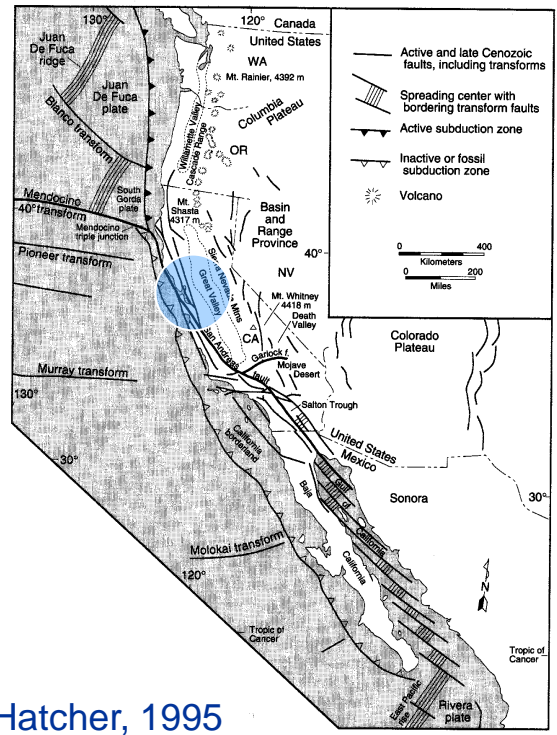


Da Mercier & Vergely, 1996

(a)

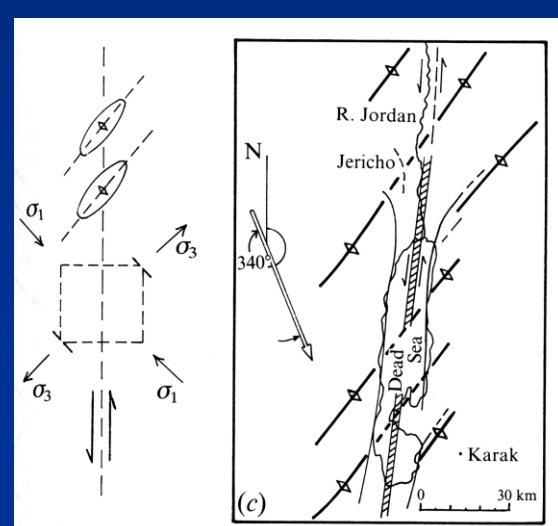


(c)



Da Hatcher, 1995

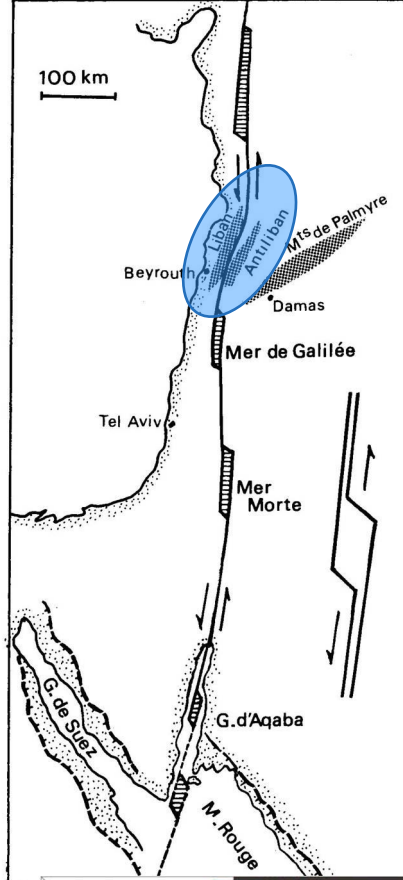
FIGURE 12-12 San Andreas and related fault systems in California, northern Mexico, and in the adjacent Pacific Ocean. (After J. C. Crowell, 1987, *Episodes*, v. 110.)



Da Price & Cosgrove, 1990

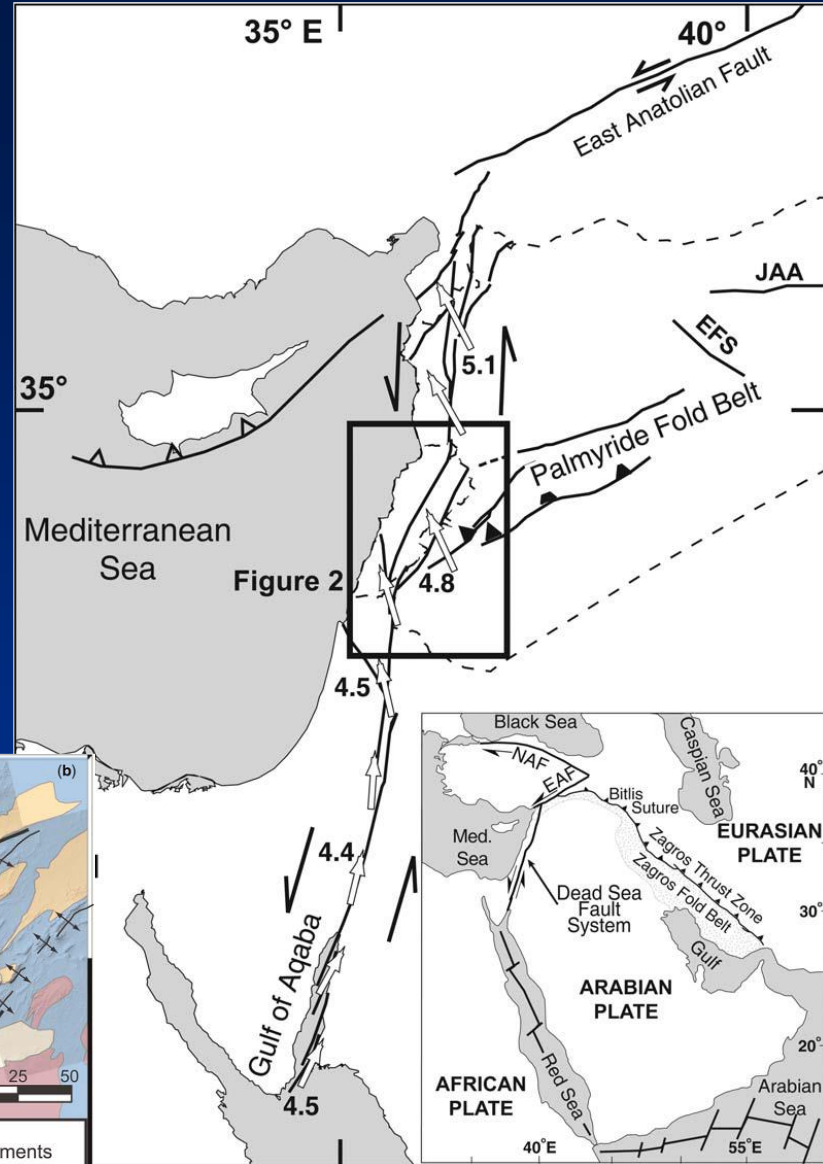
Da Hatcher, 1995

Variazioni di direzione (bend),
bacini pull-apart e faglie vicarianti (step over)

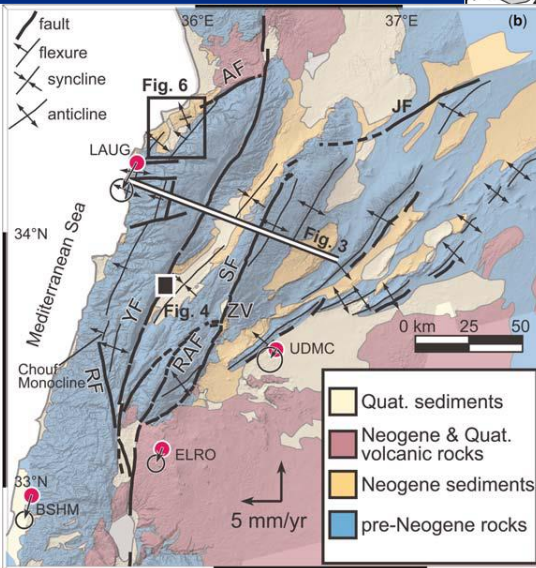
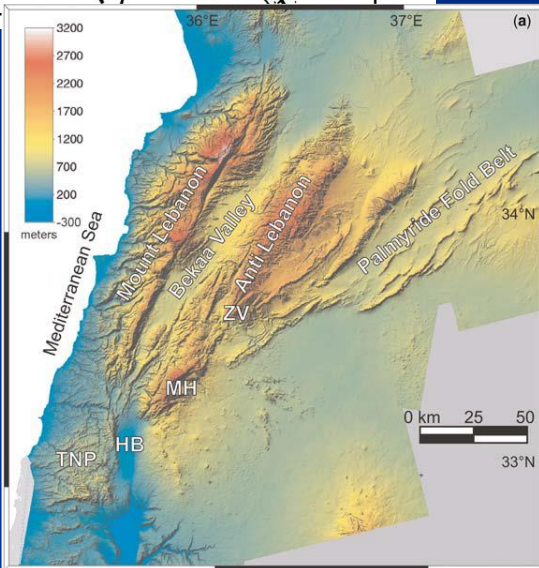


Da Debelmas et al., 2008

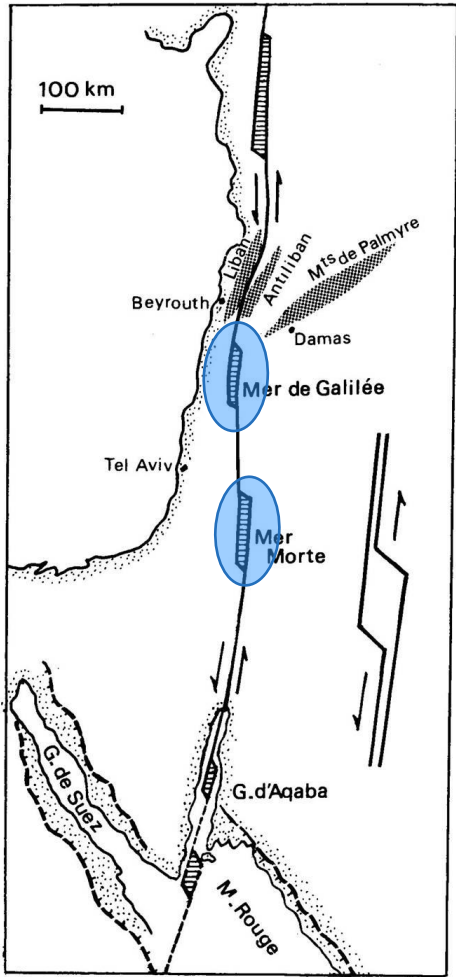
Restraining bend



Da Gomez et al., 2007

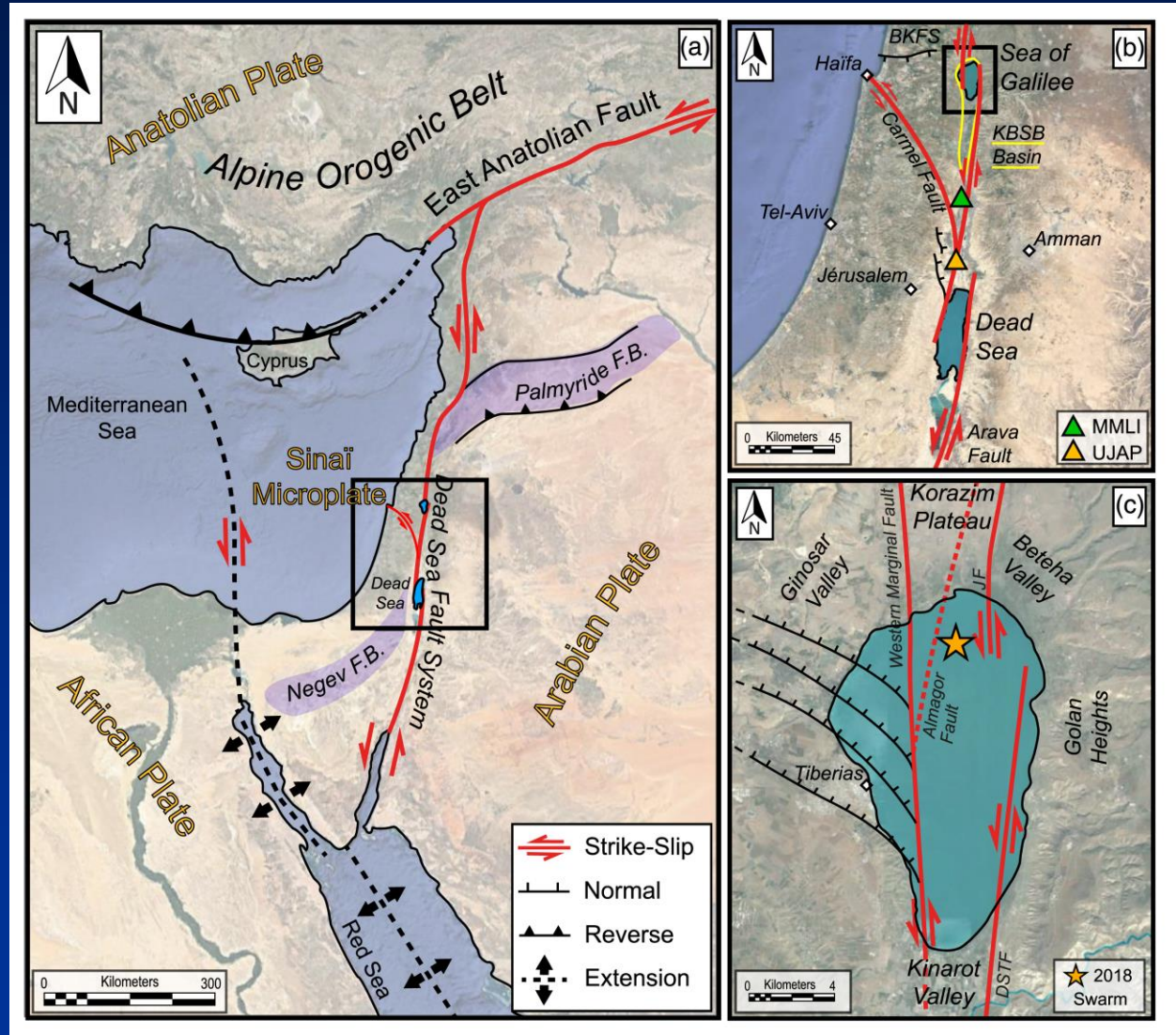


Variazioni di direzione
(bend),
bacini pull-apart e faglie
vicarianti (step over)



Da Debelmas et al., 2008

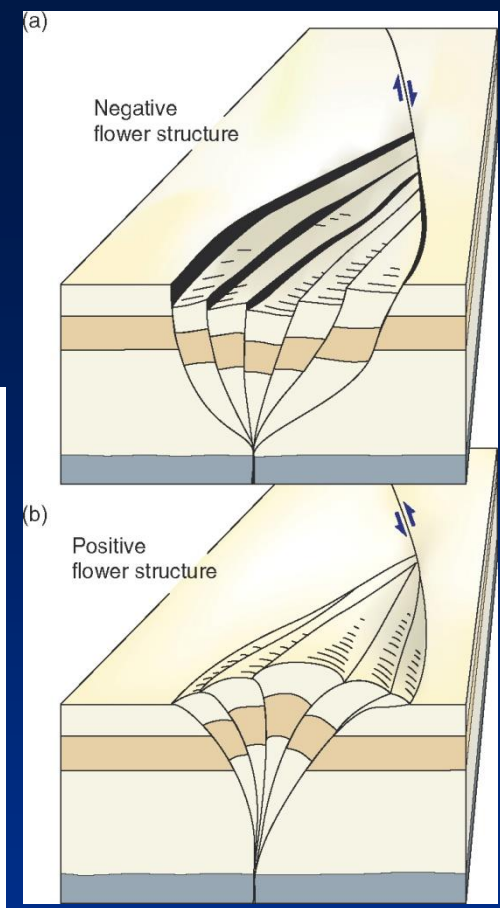
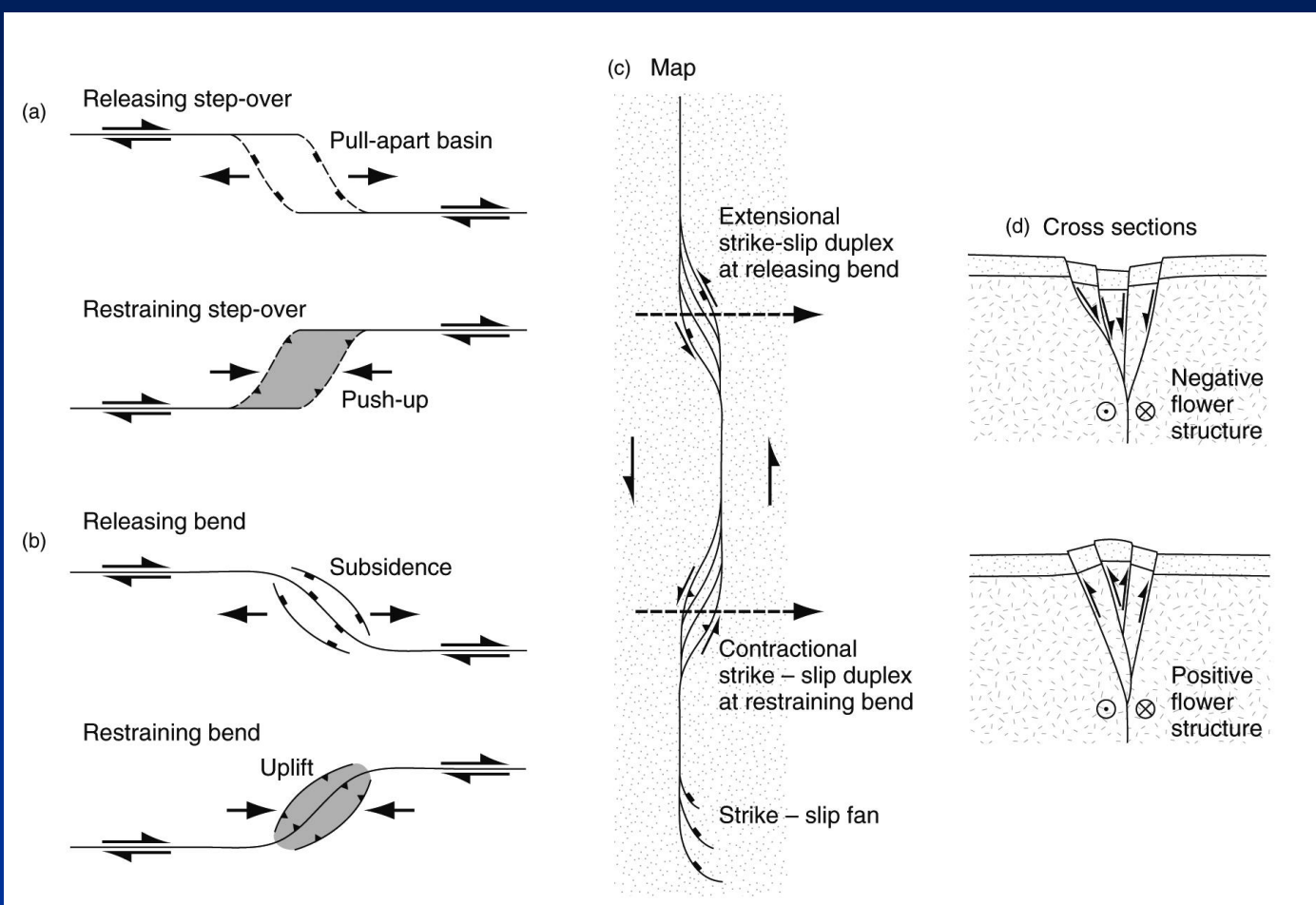
Releasing step-over – bacini pull-apart



Da Hadad et al., 2020

Variazioni di direzione (bend) e strutture a fiore

Faglie vicarianti (step-over)



•Da Fossen, 2010

Strutture a fiore

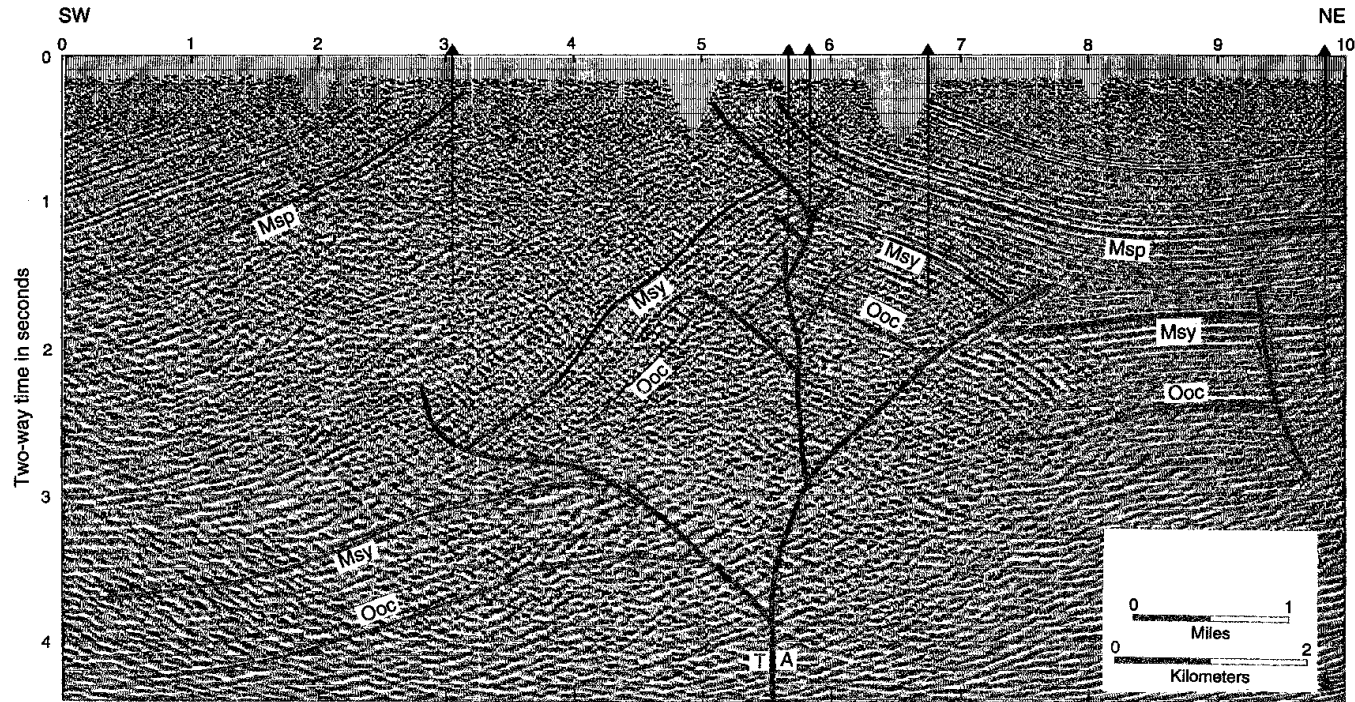
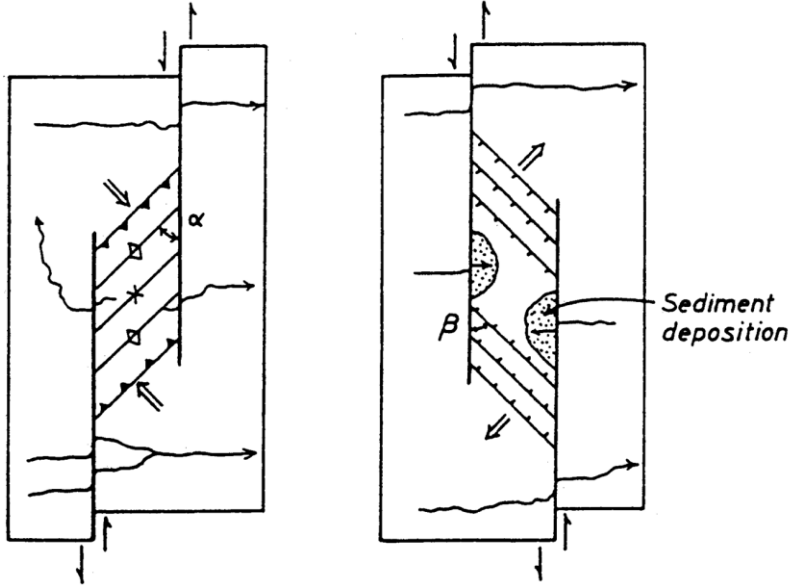


FIGURE 12-11

Structure section constructed on a seismic reflection profile and drill data through the Ardmore basin in the Oklahoma aulocogen, illustrating flower and inverted-rift structures. Msp—Springer, Msy—Sycamore, and Ooc—Oil Creek are Paleozoic rock units. (After T. P. Harding and J. D. Lowell, 1974, *AAPG Bulletin*, v. 58. Reprinted by permission of American Association of Petroleum Geologists.)

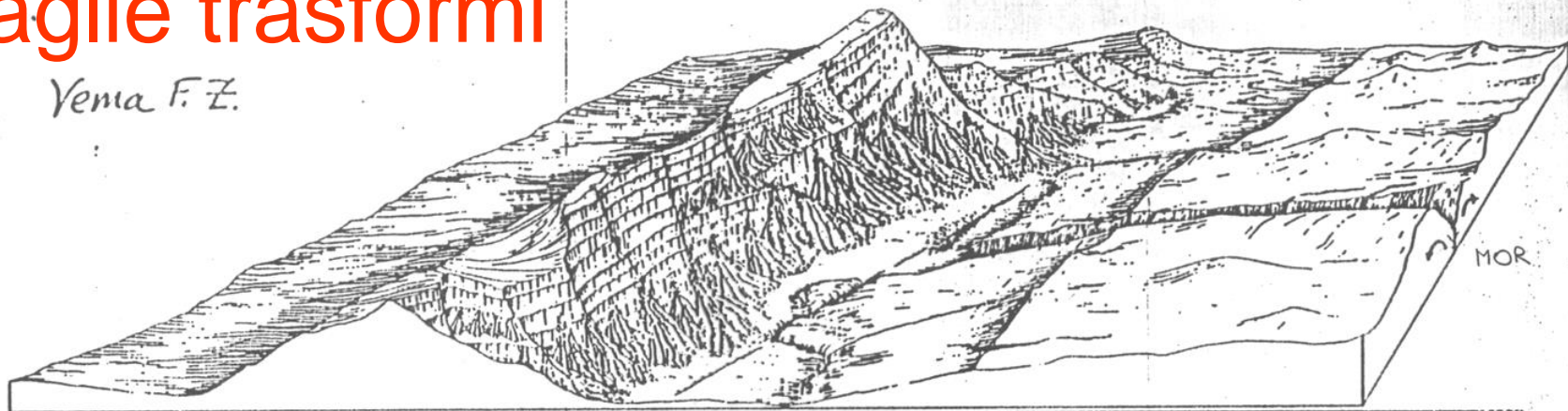
Da Ramsay & Huber, 1987

A. l.h. shear, r.h. en-echelon B. l.h. shear, l.h. en-echelon

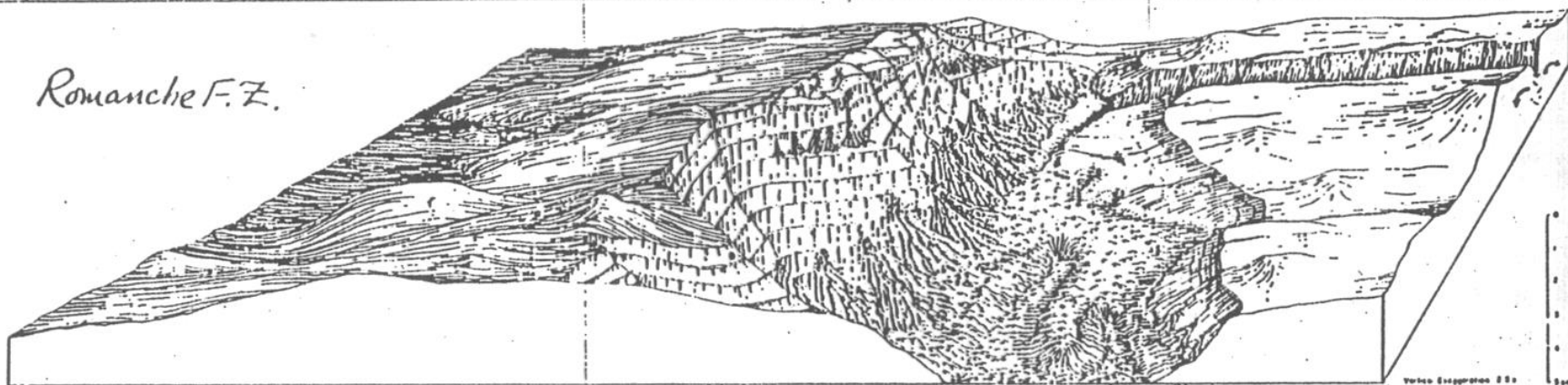


Faglie trasformi

Vema F.Z.



Romanche F.Z.



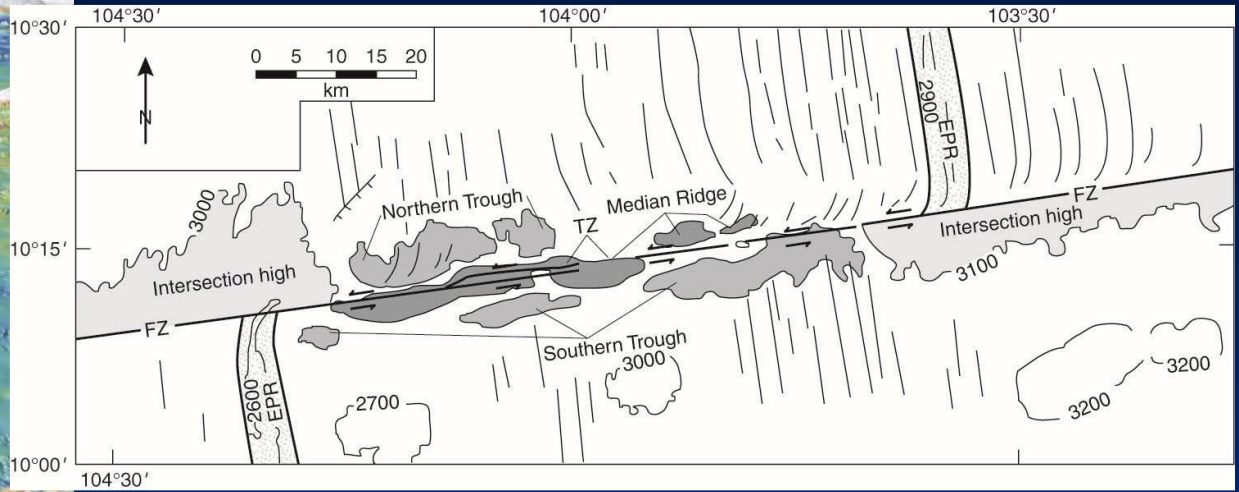
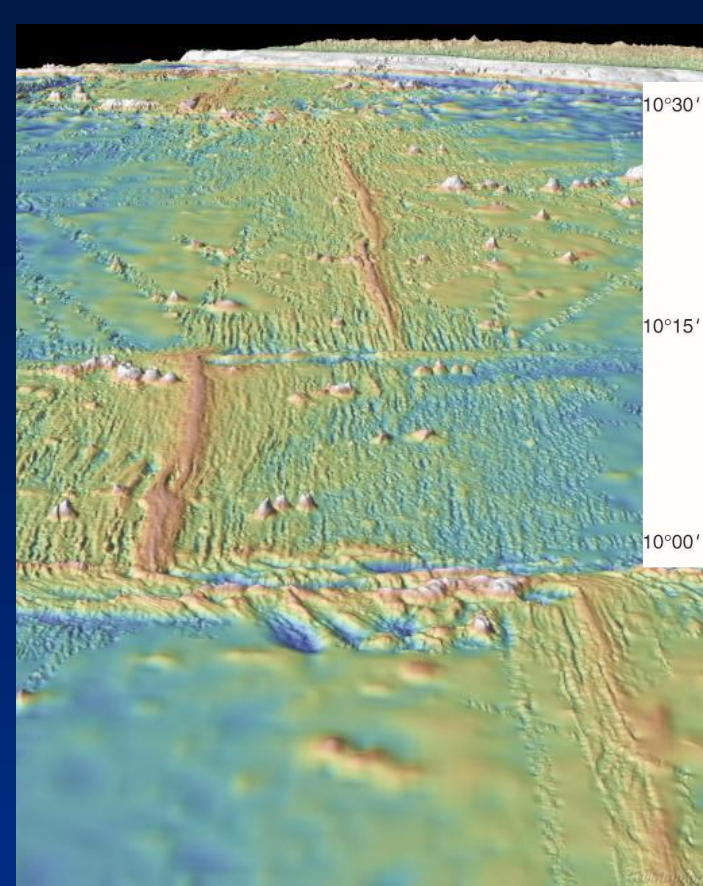
Grand Canyon



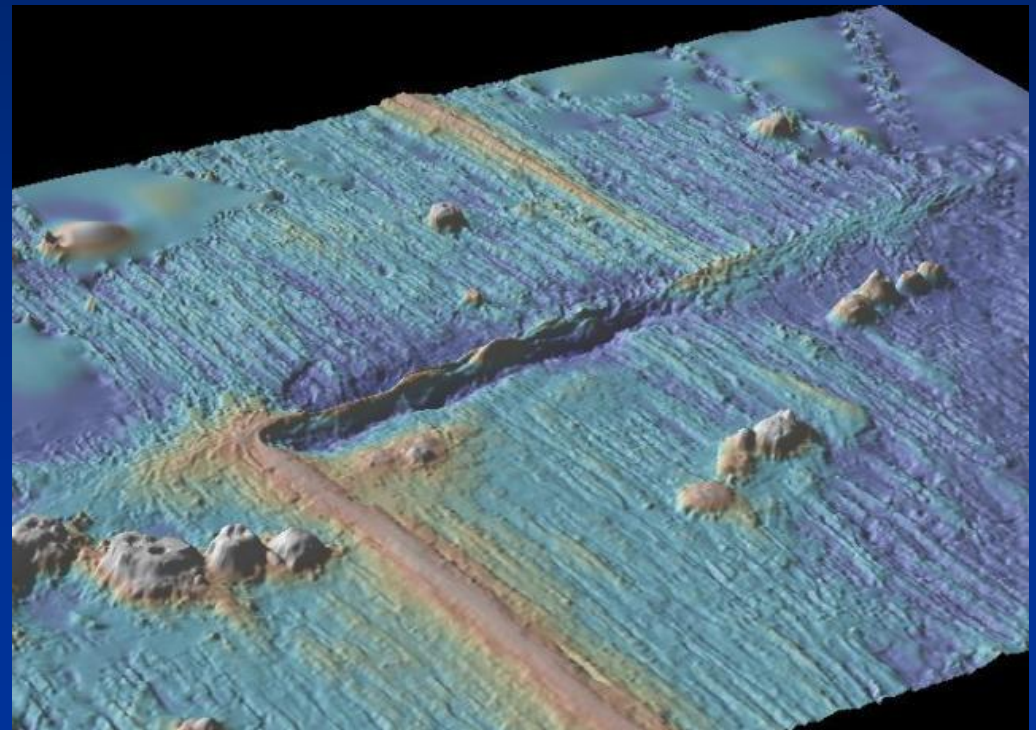
Confronto fra le
dimensioni di questo
tipodi strutture
con analoghe
subacquee.

Figure 1: Large-offset and/or slow-slipping transform faults and fracture zones rank among the major landforms of the earth. In this drawing, the transform valleys of the Vema and Romanche Fracture Zones dwarf the Grand Canyon. Such enormous relief cannot result from passive strike-slip sliding of adjacent lithospheric blocks, but rather must involve rapid and extreme vertical motions.

da KASTENS et al.
Prog. ric. 1986



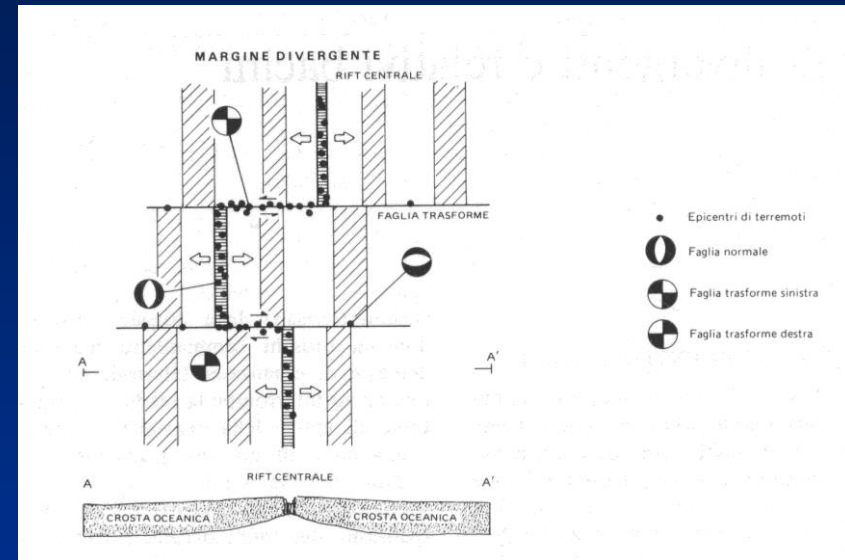
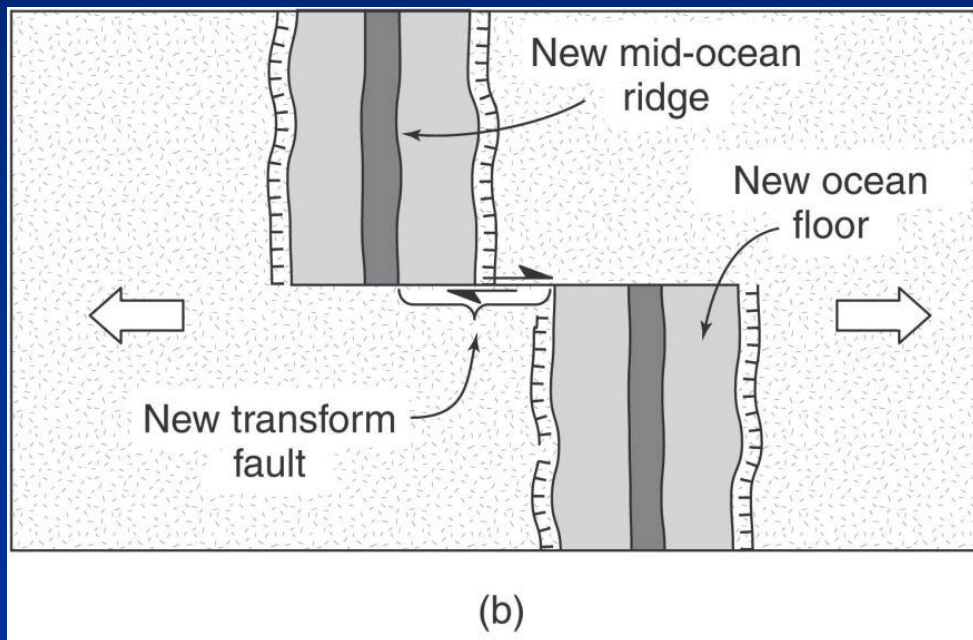
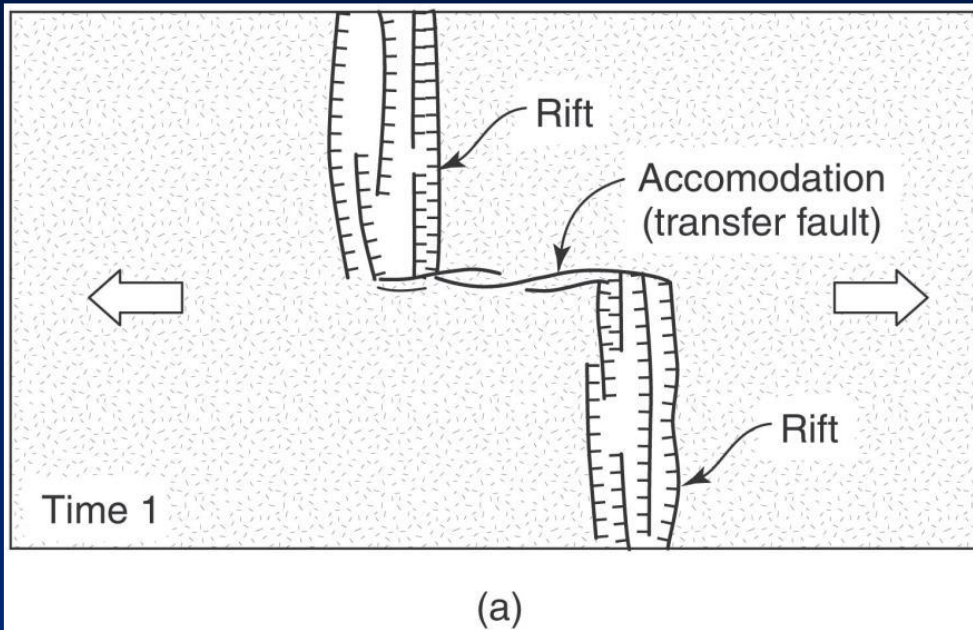
Da van der Pluijm B., Marshak S., 2004



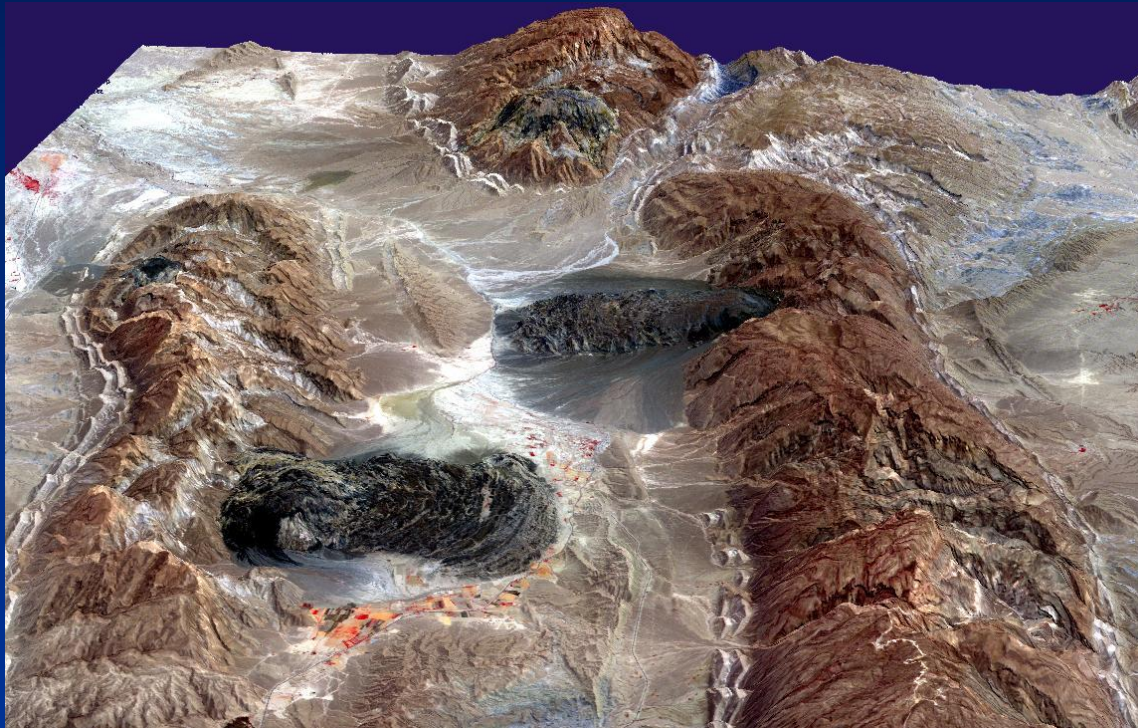
East Pacific Rise, Siqueiros and Clipperton Transform Faults
 Da MGDS Media Bank, 2007
<http://media.marine-geo.org/image/>

Clipperton Transform Fault
 Da MGDS Media Bank, 2007
<http://media.marine-geo.org/image/>

Faglie trasformi



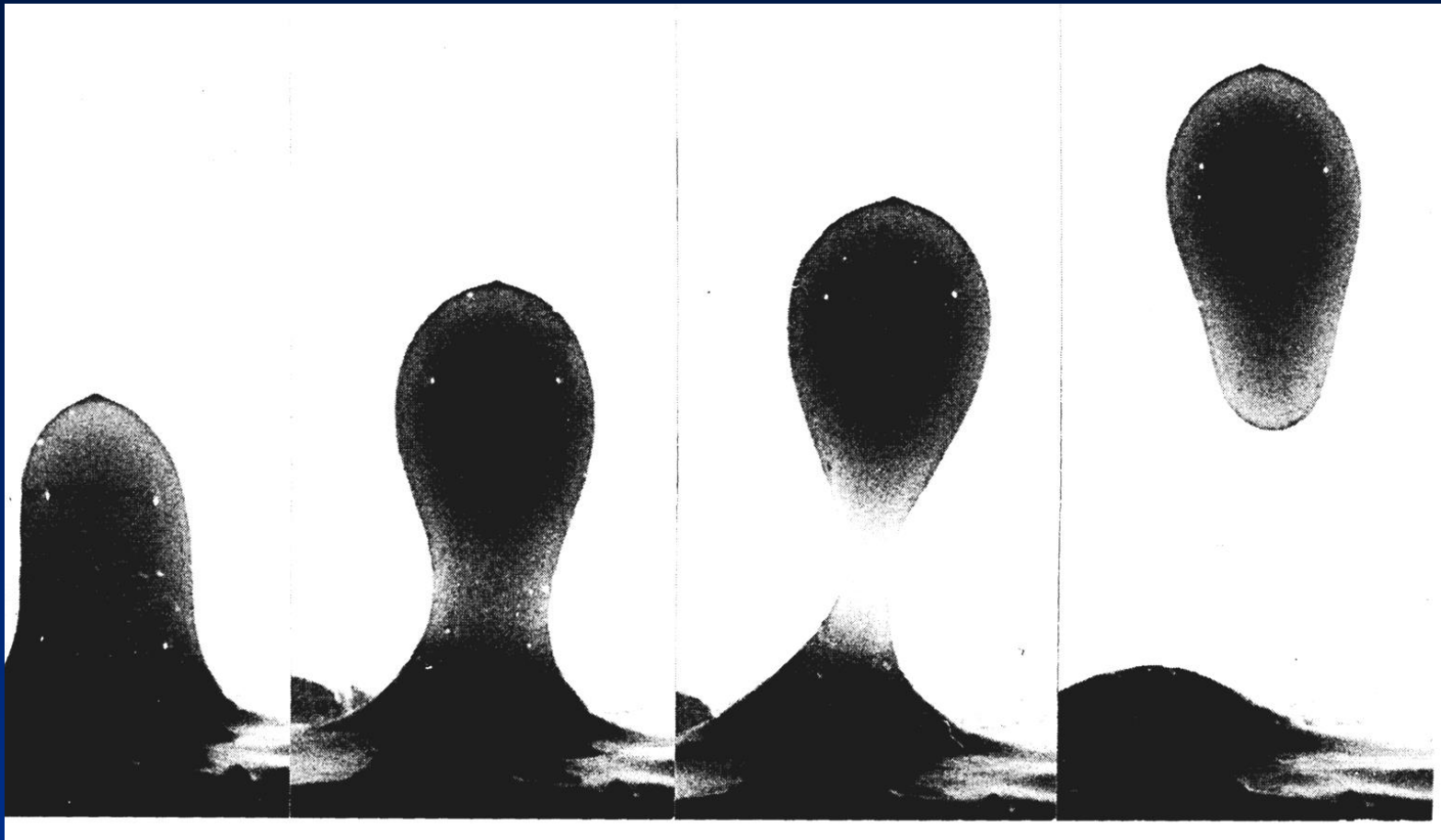
Tettonica diapirica



Salt glacier da diapiri salini

Da Earth observatory NASA

Immagine da NASA/GSFC/MITI/ERSDAC/JAROS, and U.S./Japan
ASTER Science Team



Da Price & Cosgrove, 1990

Si innesca per differenziale di carico quando si attua inversione di densità in profondità. Esempio di risalita di gocce meno dense del liquido chiaro.

Tettonica diapirica

Salgemma = diapirismo o halocinesi, legata alla densità e alla mobilità del salgemma.

Gesso = diapirismo reale?, legato alla densità, ma mobilità del gesso è limitata (roccia fragile, sino a quando non si trasforma in anidrite), con sensibile influenza della sovrappressione dei fluidi interstiziali.

Fango = “pseudodiapirismo” governato da sovrappressione dei fluidi interstiziali.



Image © 2011 GeoEye
Image © 2011 DigitalGlobe
Data SIO, NOAA, U.S. Navy, NGA, GEBCO
© 2011 Cnes/Spot Image
27°17'24.43" N 54°38'29.65" E elev 1661 ft

© 2010 Google

Eye alt 154.27 mi



Image © 2011 GeoEye
Image © 2011 DigitalGlobe

© 2010 Google

Imagery Dates: Mar 13, 2006 - Sep 6, 2009

© 2011 Cnes/Spot Image
27°56'19.95" N 64°54'22.65" E elev 2309 ft

Eye alt 26.96 mi

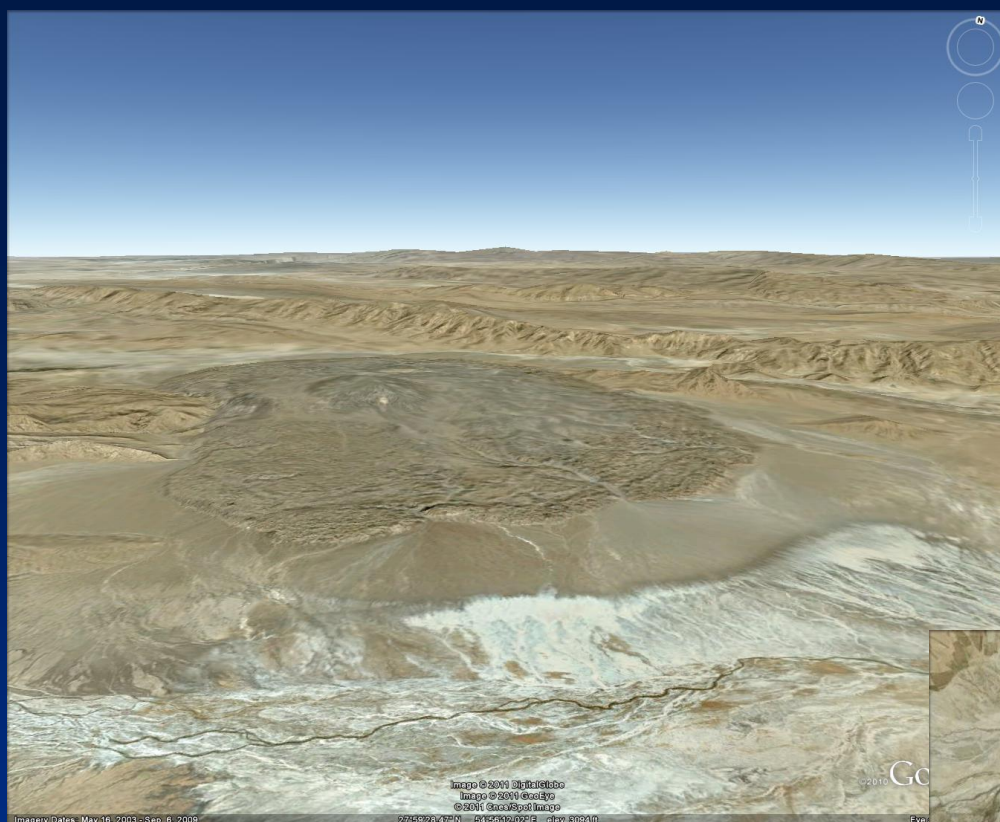


Image © 2011 DigitalGlobe
Image © 2009 GeoEye
© 2011 CoreSpot Image

Google

Imagery Dates: May 16, 2003 - Sep 6, 2009

57°59'28.47"N 63°56'12.02"E elev 8392m

Eye alt



Image © 2011 DigitalGlobe
Image © 2009 GeoEye
© 2011 CoreSpot Image

Google

Imagery Dates: Mar 13, 2006 - Sep 6, 2009

28°00'00.95"N 94°54'39.91"E elev 4281m

Eye alt: 10684m

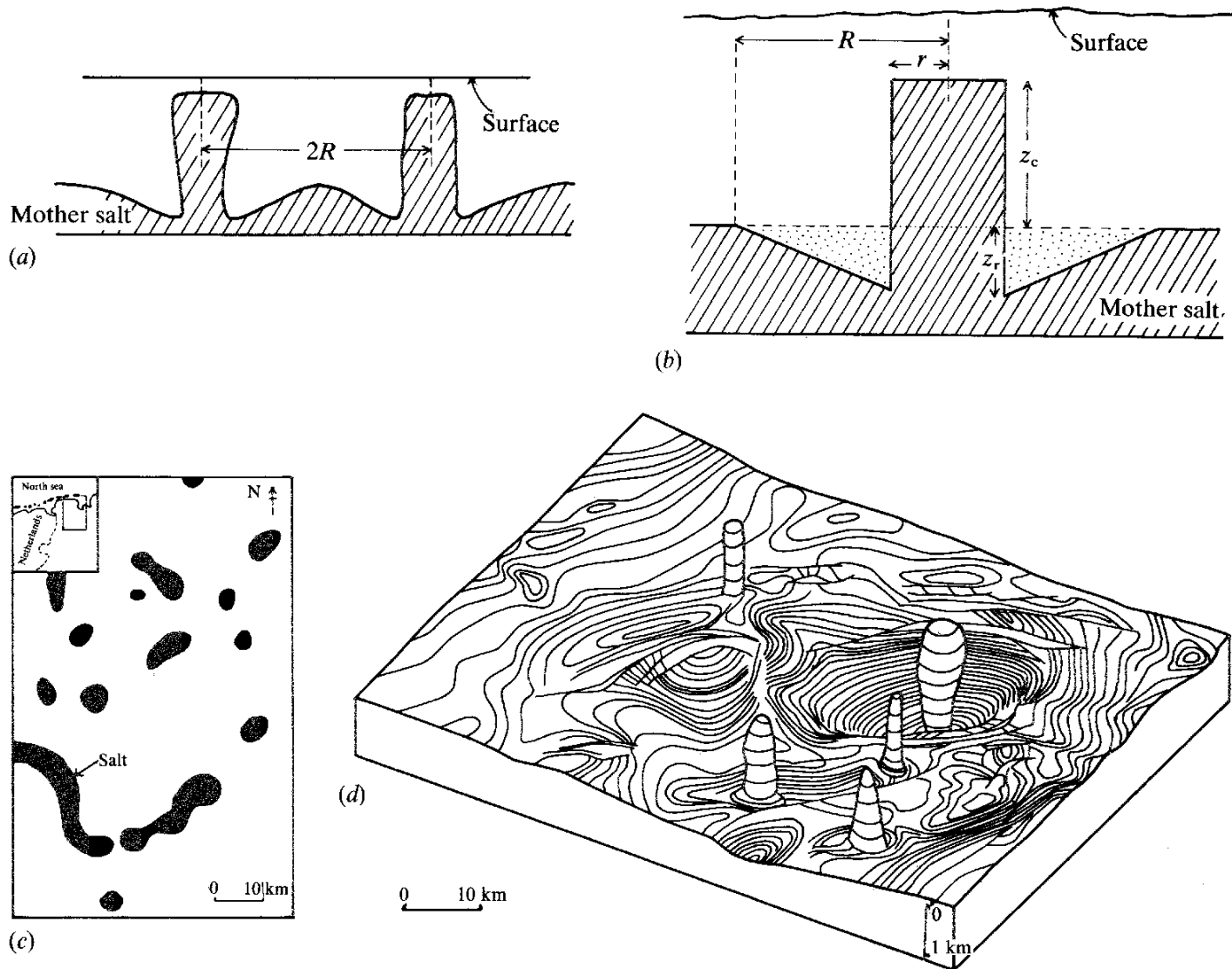
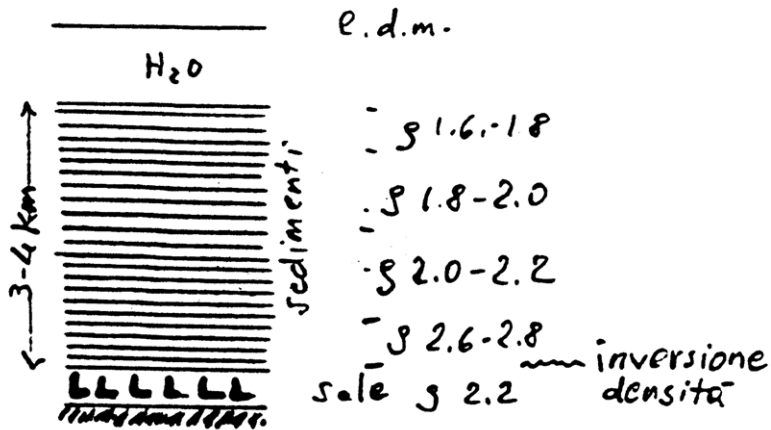
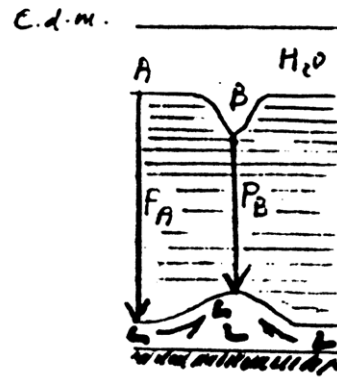


Fig. 4.13. (a) Schematic representation of section through two adjacent, bollard-type plugs. (b) Simplified geometry of salt layer and plug. (c) Distribution of Salt Domes in a small area of N. Germany. (After Turcotte & Schubert, 1982.) (d) Block diagram of salt plugs piercing the top of the Woodbine whose structure contours are shown. (After Jackson & Seni, 1983.)

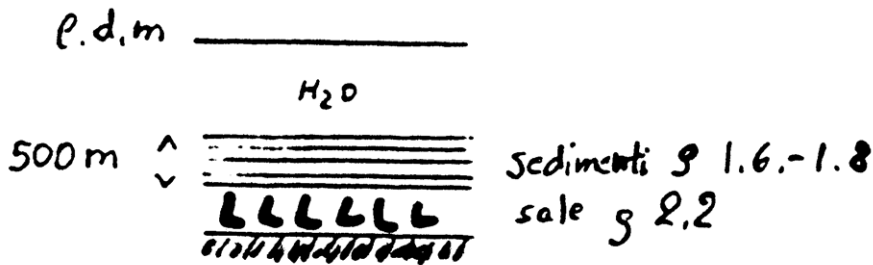


② CONDIZIONI DI HALOCINESI POTENZIALE



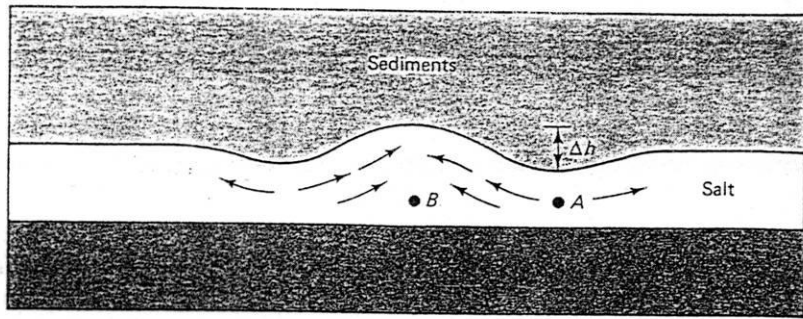
③ CONDIZIONI DI HALOCINESI EFFETTIVA (differenza di carico litostatico $P_B < P_A$ ad es. per formazione di canyon erosivo)

Fig. 190 - ①, ②, ③. Condizioni meccaniche per la formazione di diapiri

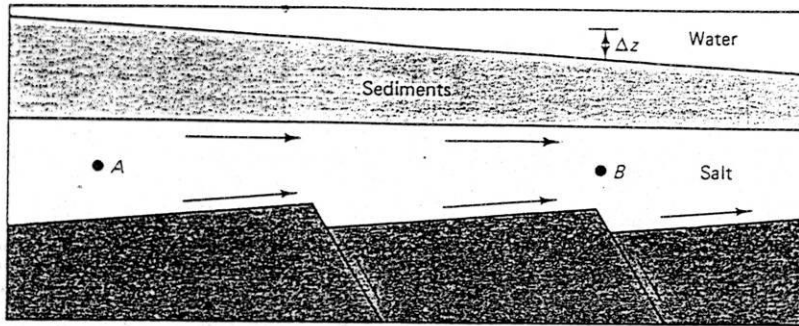


① NO HALOCINESI

Da Selli L., appunti dalle lezioni di Geologia Strutturale

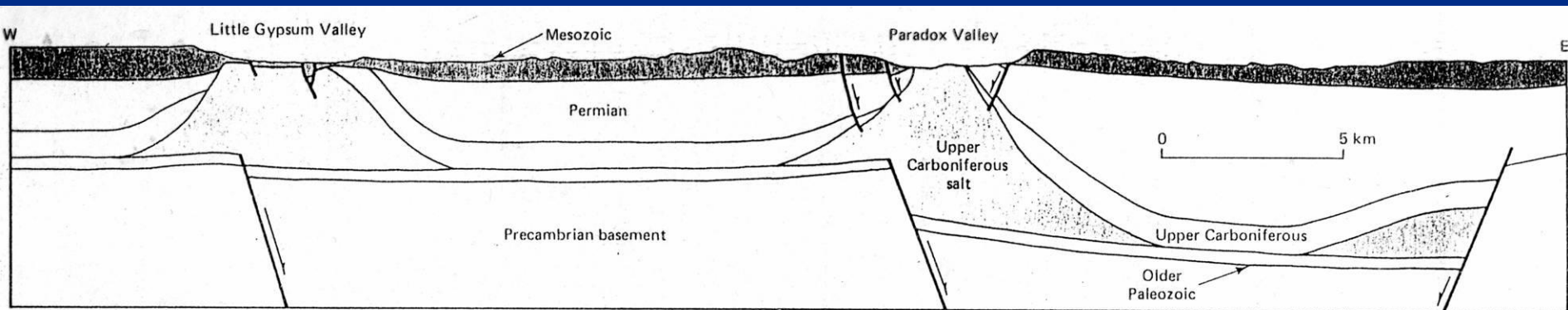


(a)



Migrazione del sale
verso le zone con meno
carico litostatico

Da Suppe, 1985



Da Suppe, 1985

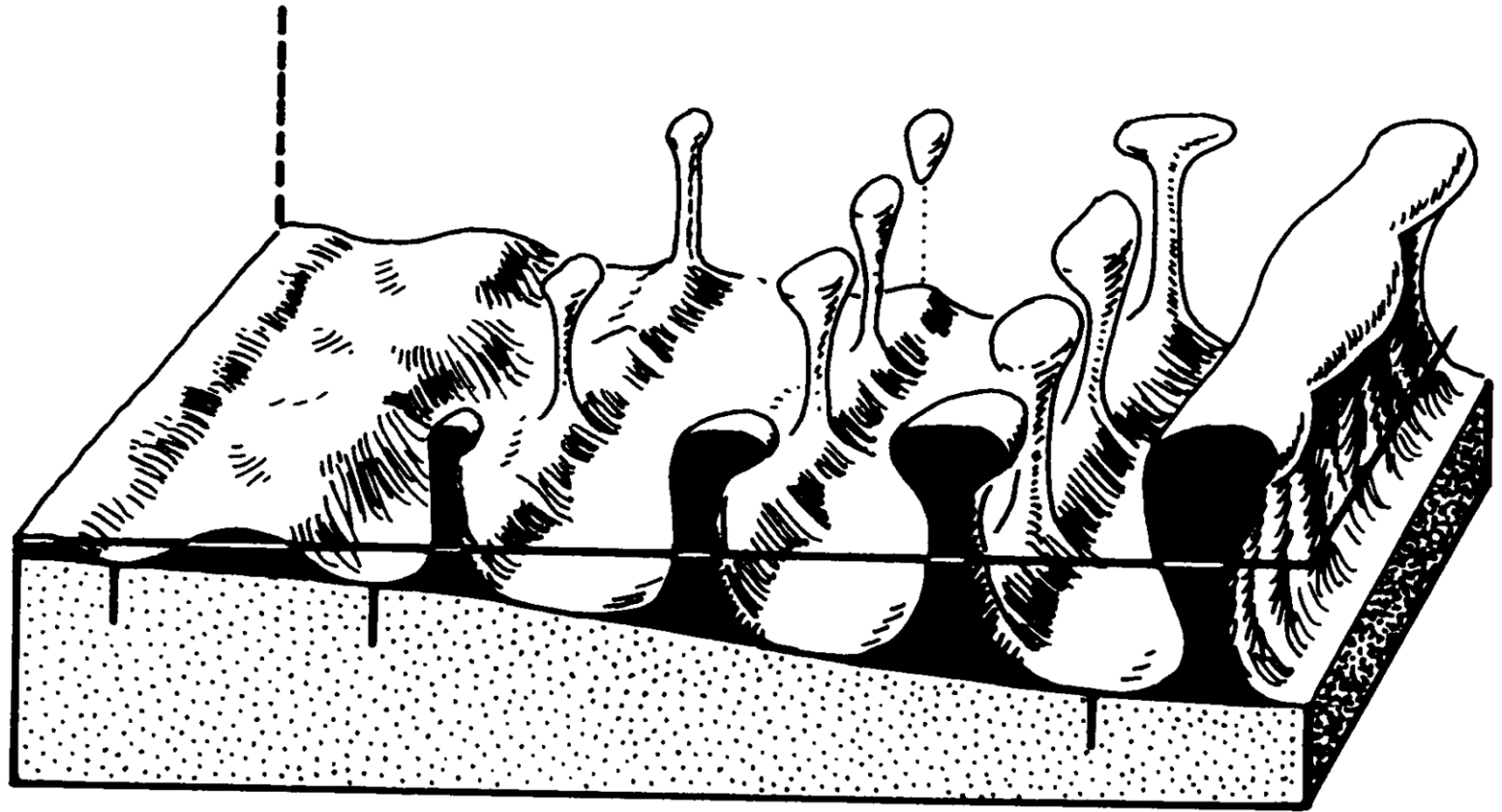
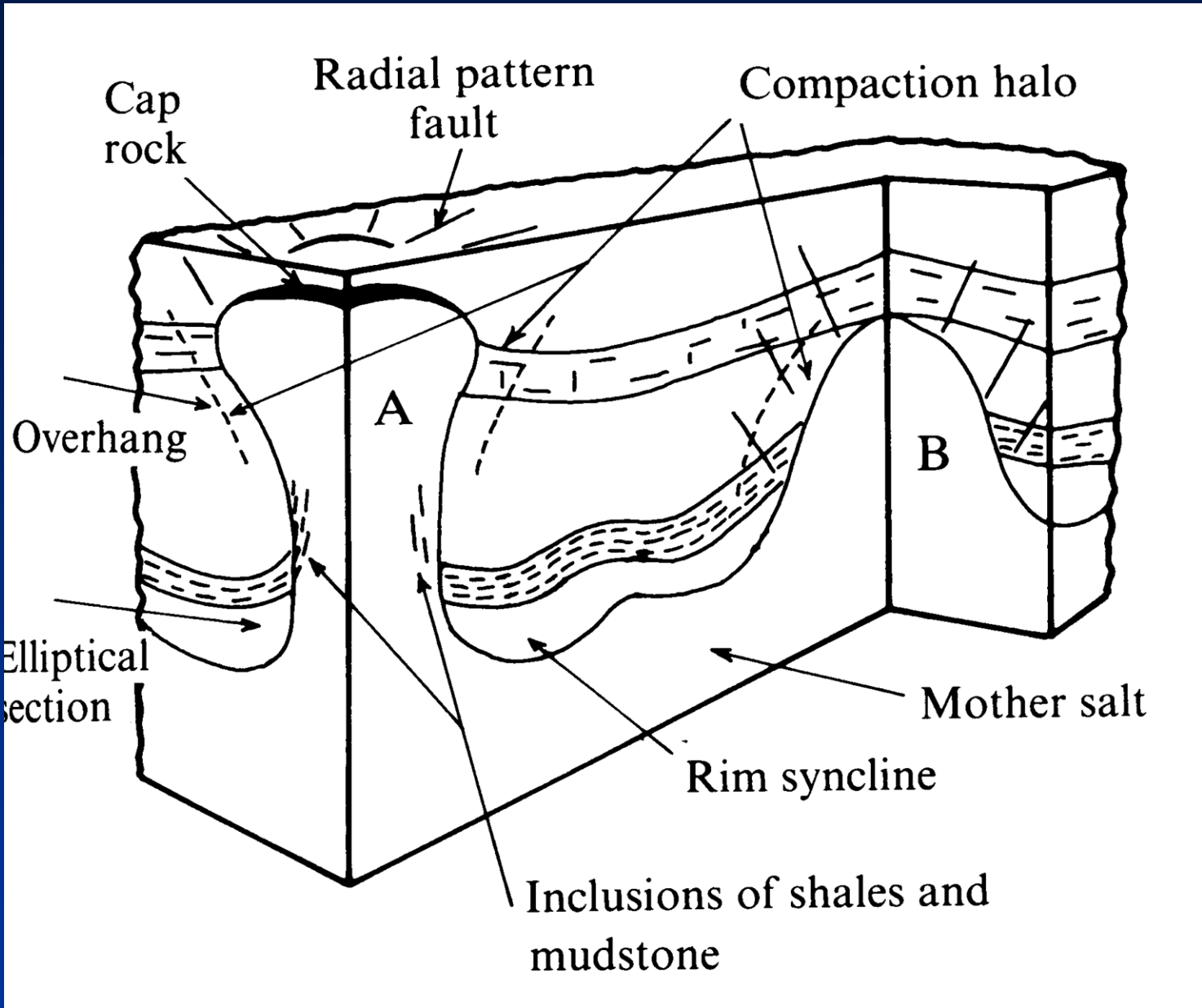


Fig. 4.7. General morphology of salt pillows, walls and domes.
(After Trusheim, 1960.)

Da Price & Cosgrove, 1990

Densità del salgemma 2,16
gesso 2,3



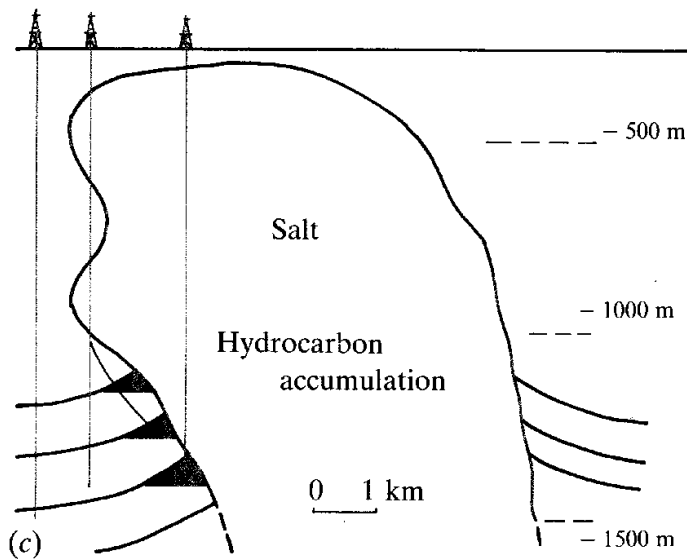
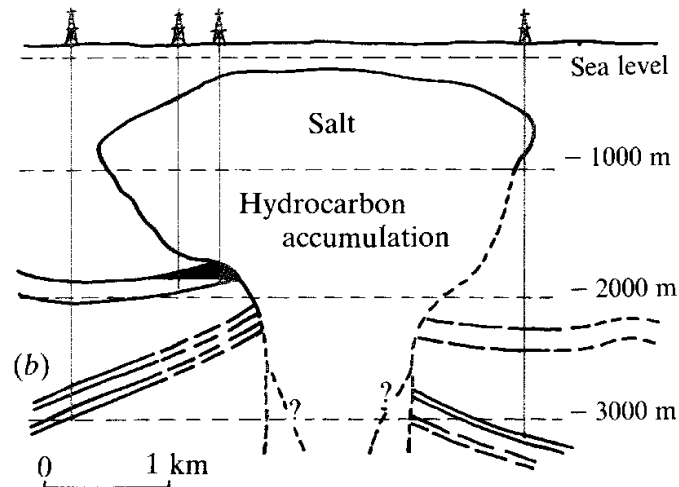
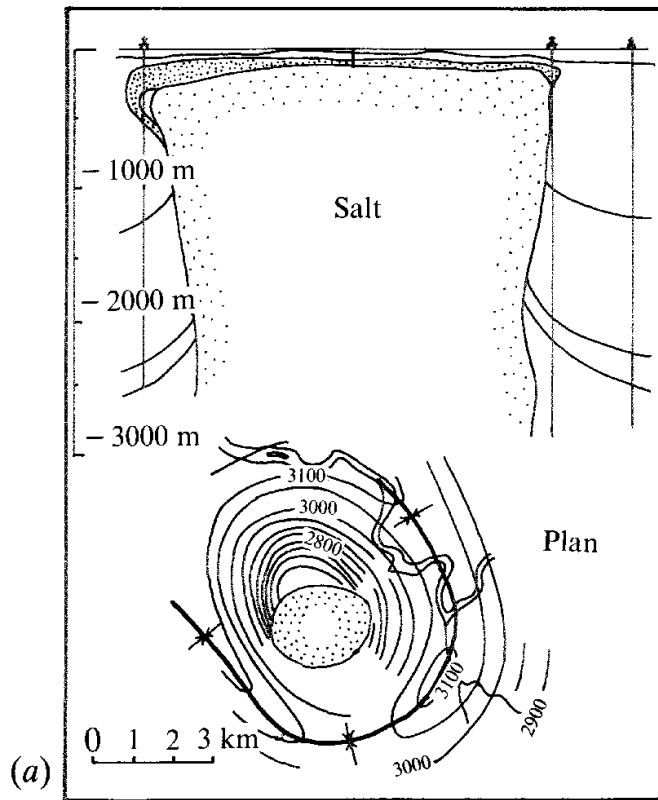


Fig. 4.8. Profiles indicating morphology of a variety of real salt domes or plugs (a) Zanapa Dome, Mexico. (b) Bethel Dome, Texas, U.S.A. (c) Cote-blanche Dome, Louisiana, U.S.A. ((b) and (c) after Halbouty, 1967).

Trappole per
idrocarburi

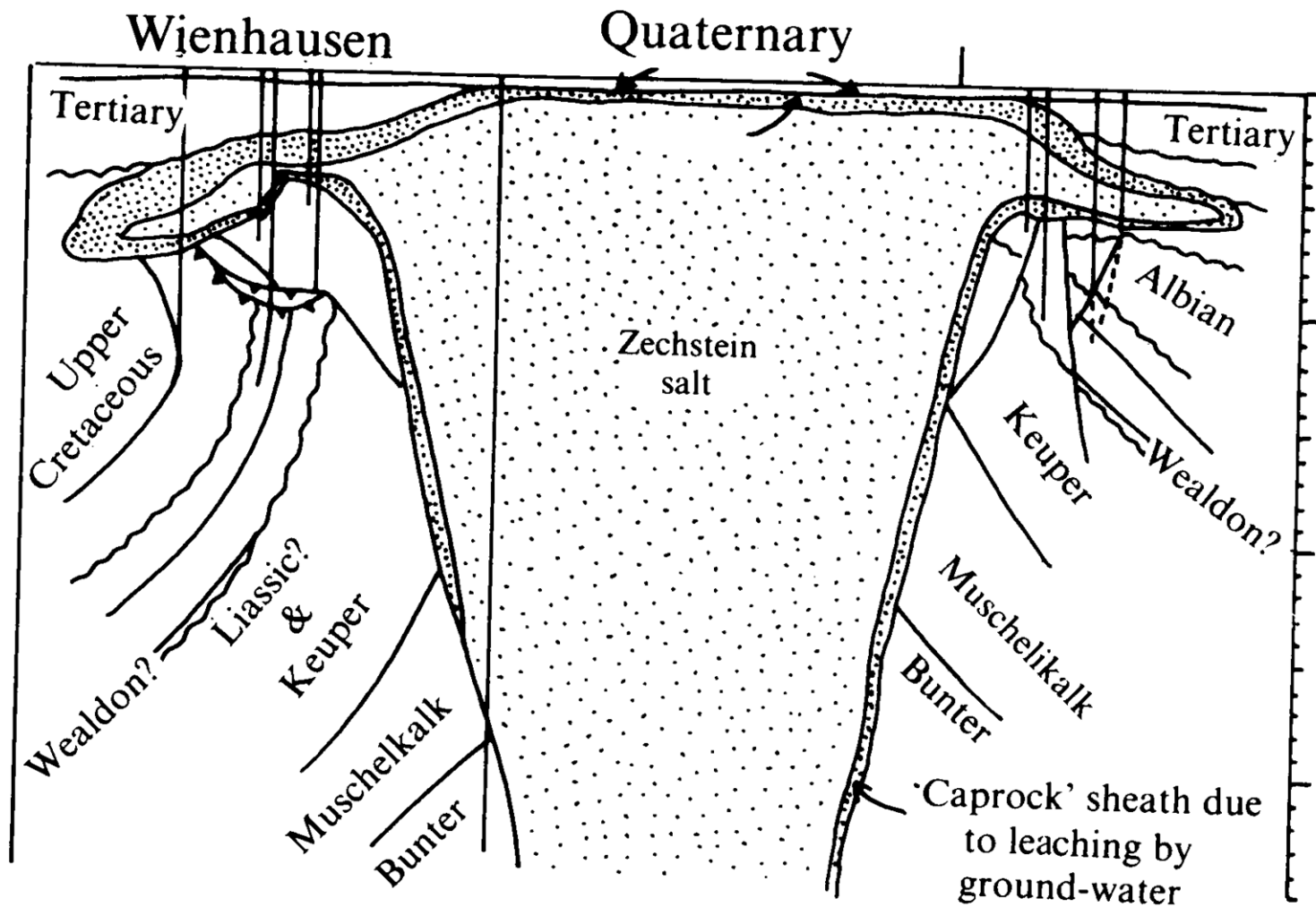


Fig. 4.25. Section through the Wienhausen Salt Plug, N.W. Germany. (From Gussow, 1968; after Schott, 1956.)



. 4.10. Sketch of vertically plunging folds revealed in the galleries of a salt mine. (After Balk, 1953.)

Da Price & Cosgrove, 1990



Image © 2011 DigitalGlobe
Image © 2011 GeoEye
© 2011 Cnes/Spot Image

Imagery Dates: Mar 13, 2006 - Sep 6, 2009

28°00'00.95" N 54°54'35.91" E elev 4281 ft

Eye alt 10.84 mi

Vulcani e diapiri di fango, grifoni, salse

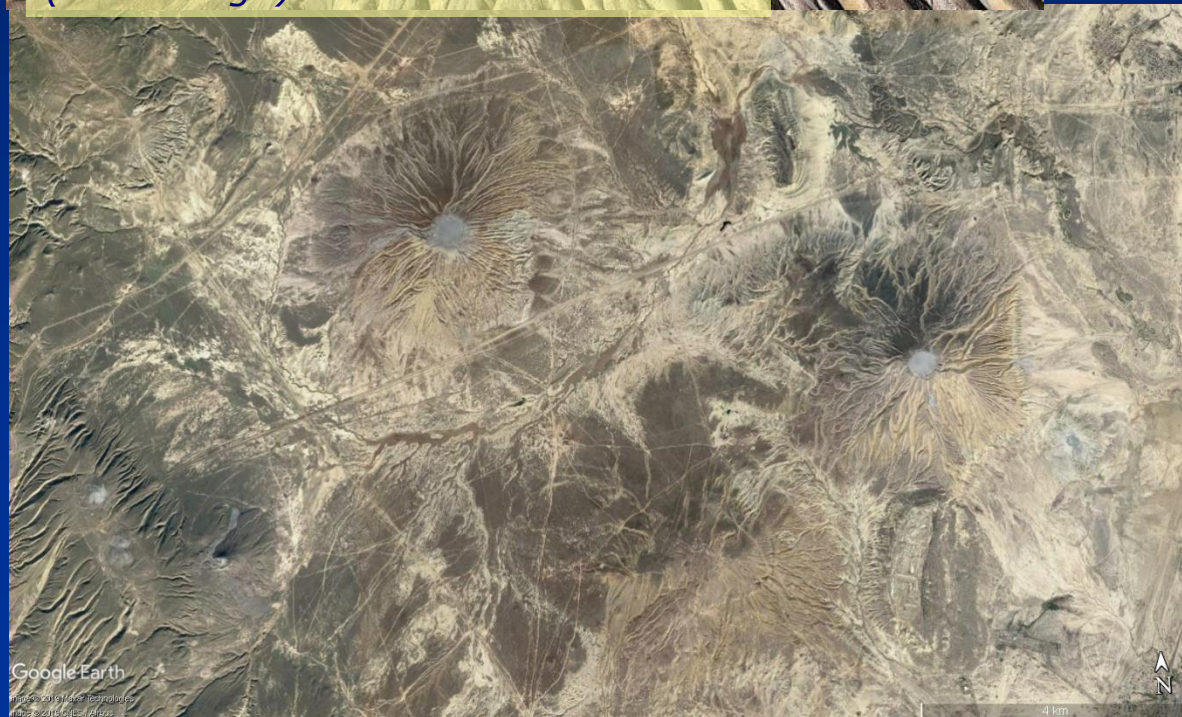




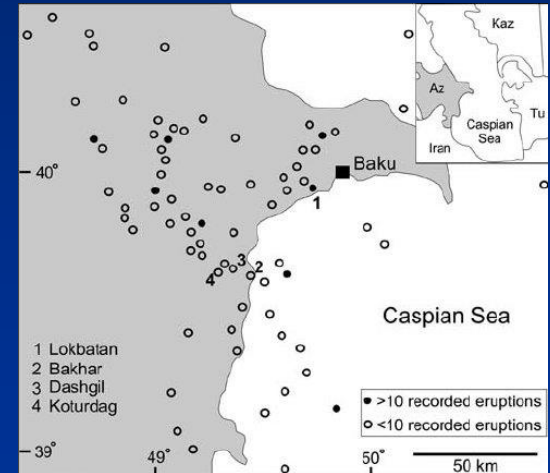
Toragai mud volcano, Azerbaijan
(500 m high)



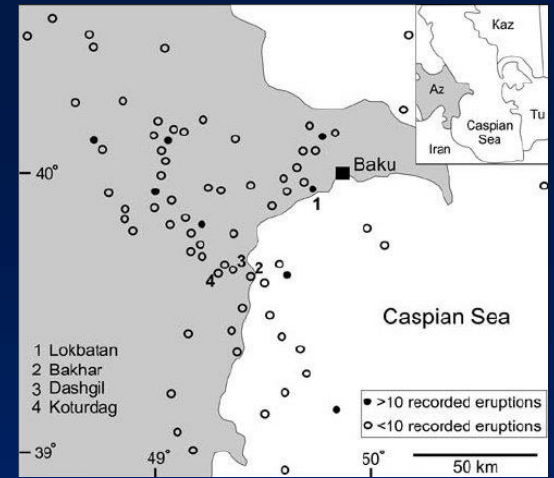
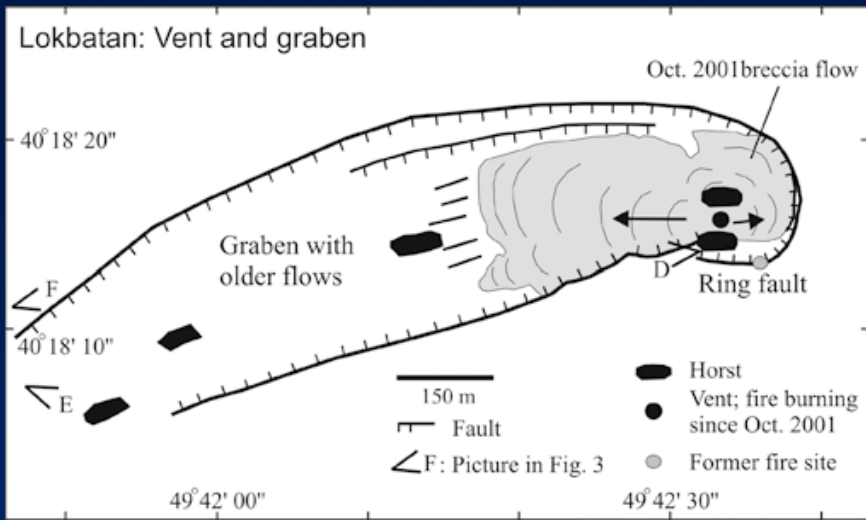
Da Phil Hardy, BBC, 2001



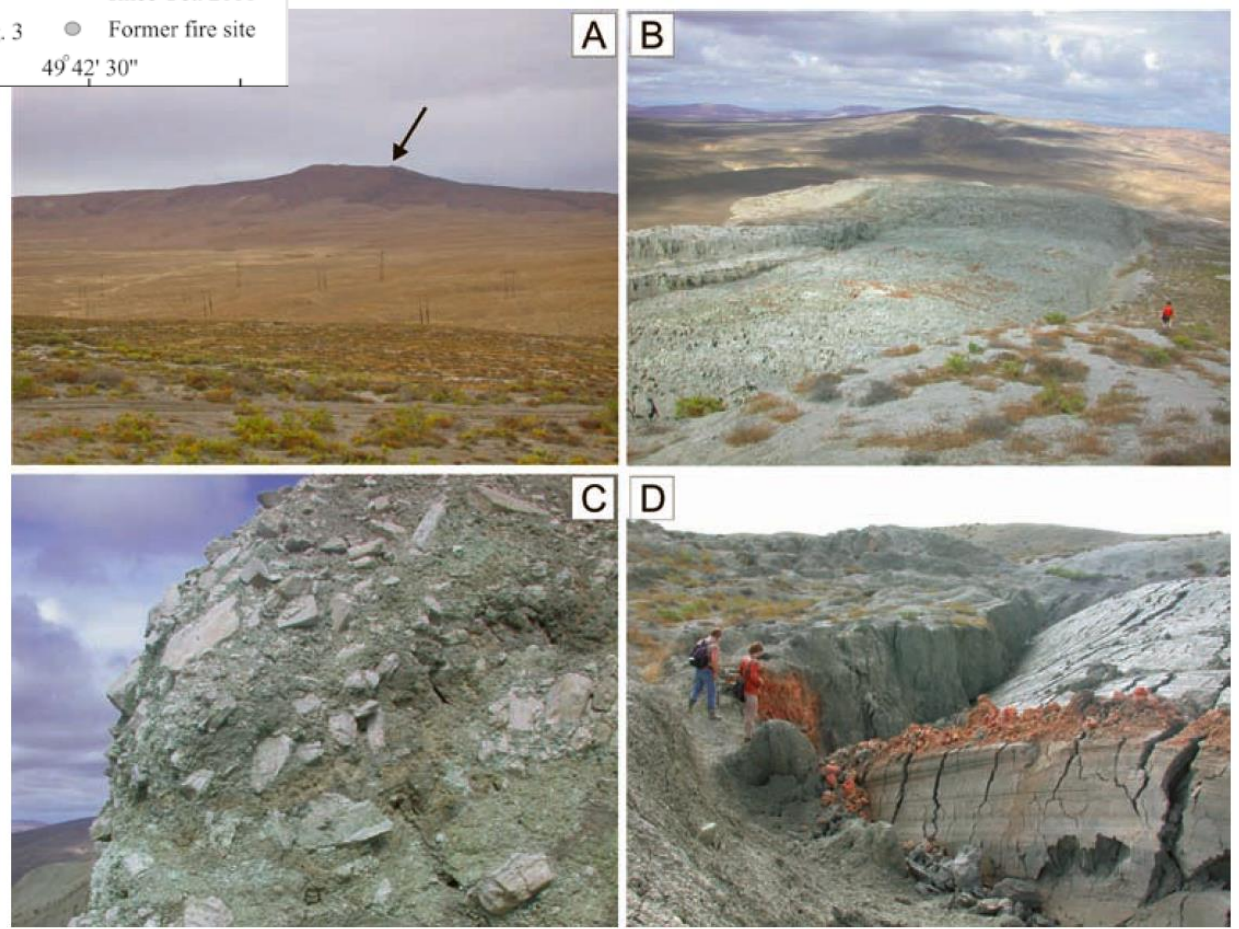
Google Earth



Qobustan National
Park, Azerbaijan

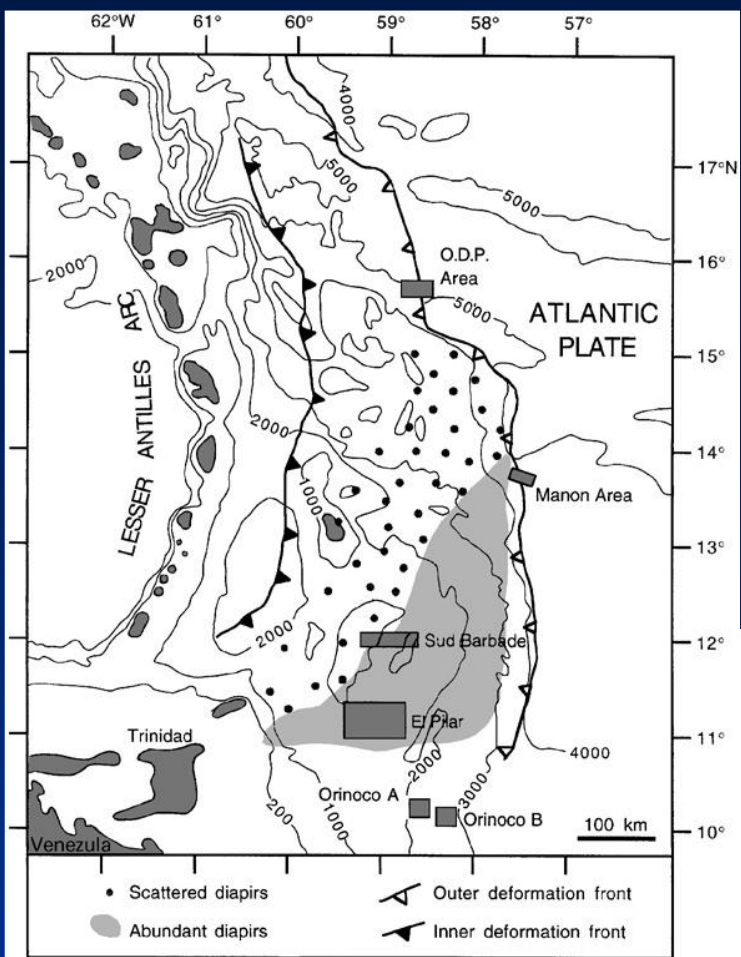


Da Planke et al., 2003

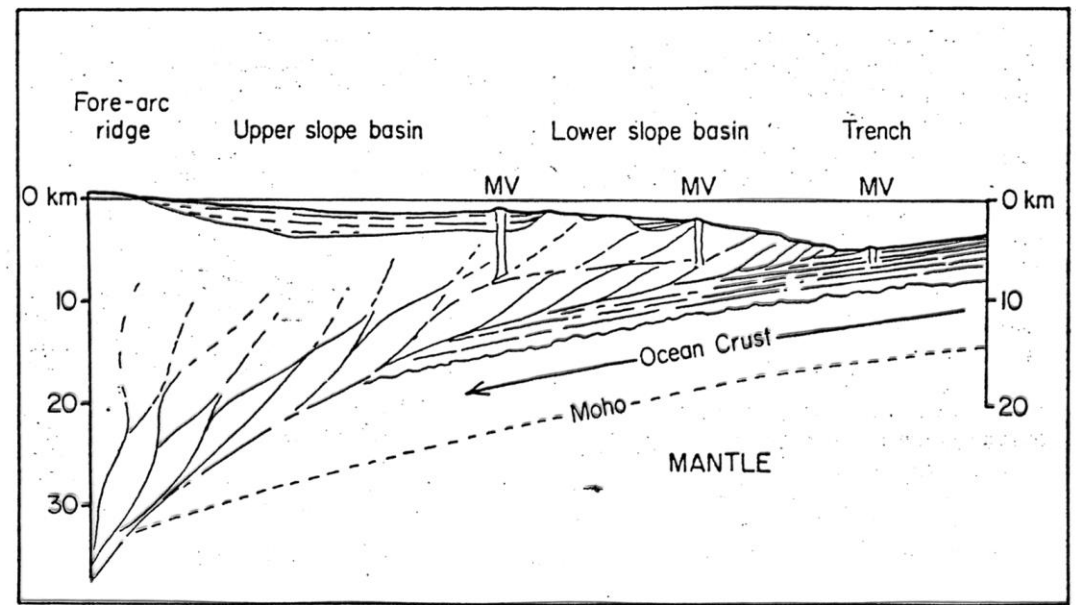


Qobustan National
Park, Azerbaijan

Vulcani di fango nel prisma di accrezione, Barbados

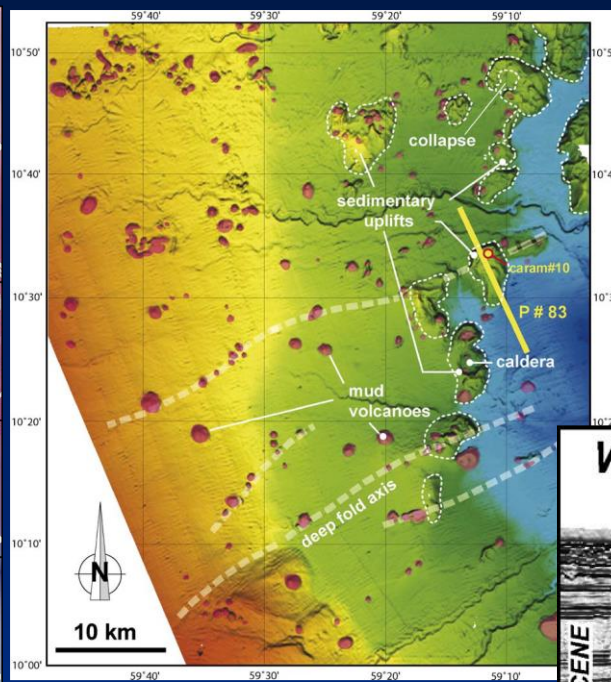
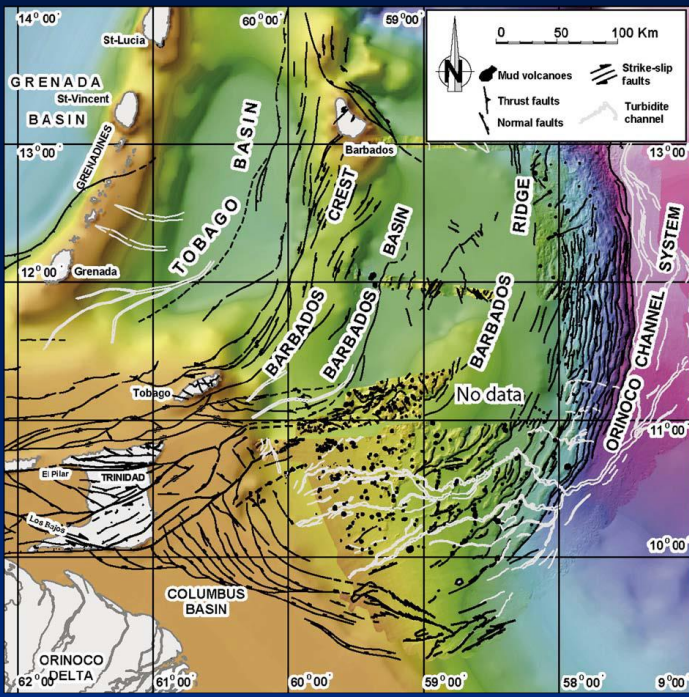


Da Aloisi et al., 2002

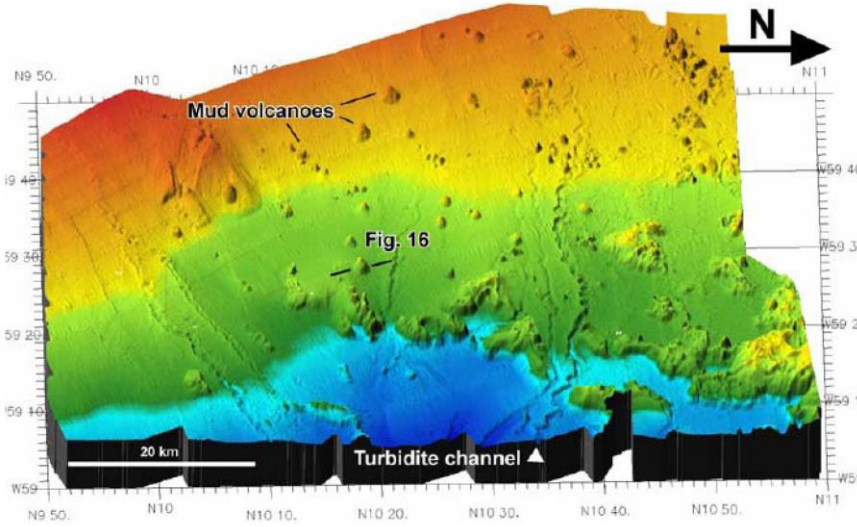
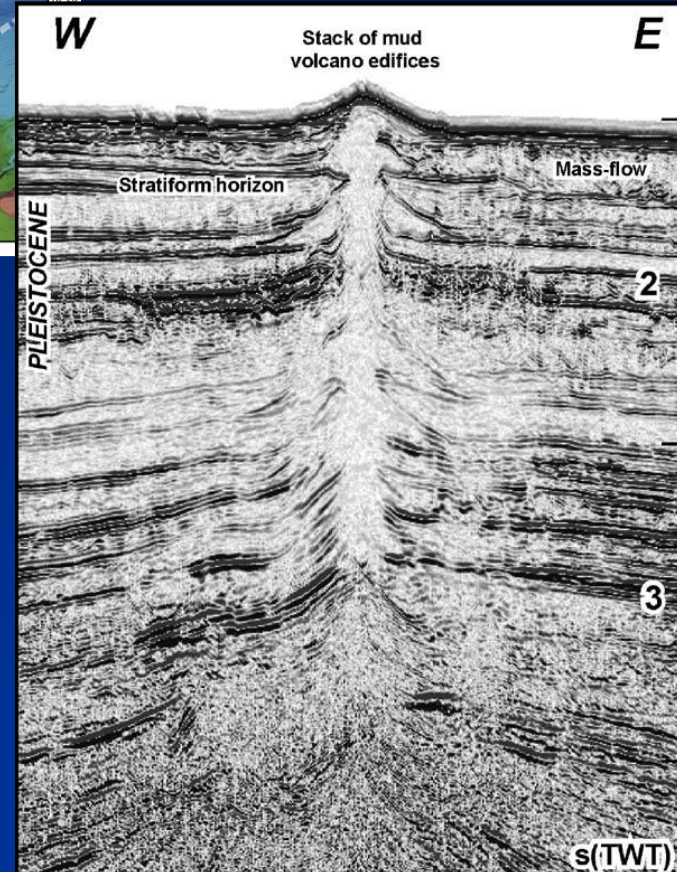


Da Barber & Brown, 1988

Vulcani di fango nel prisma di accrezione, Barbados



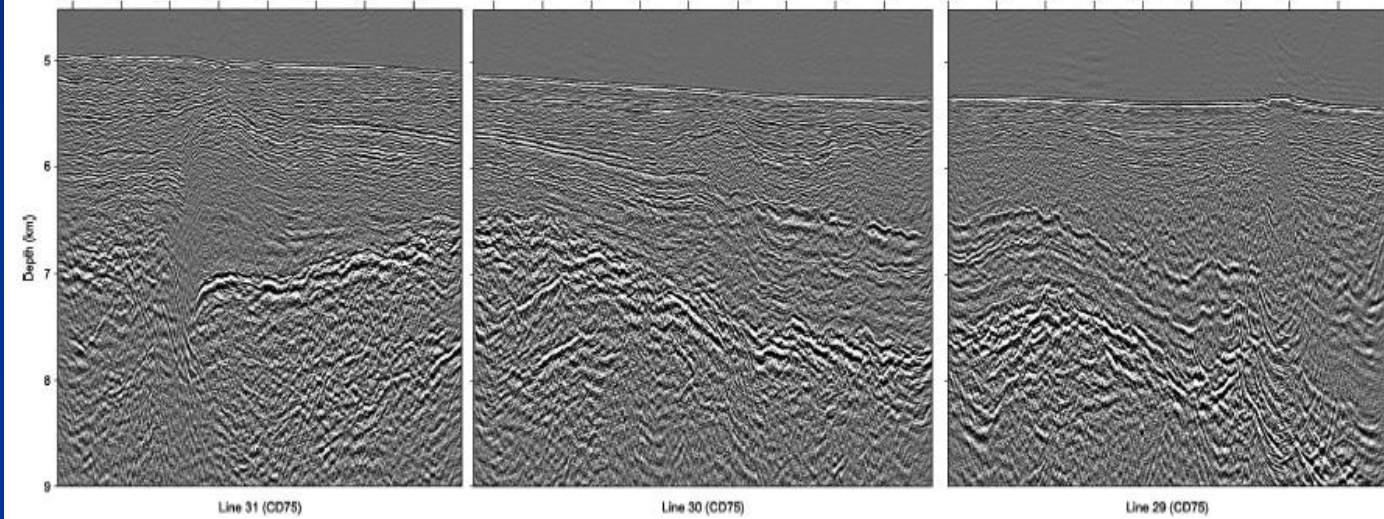
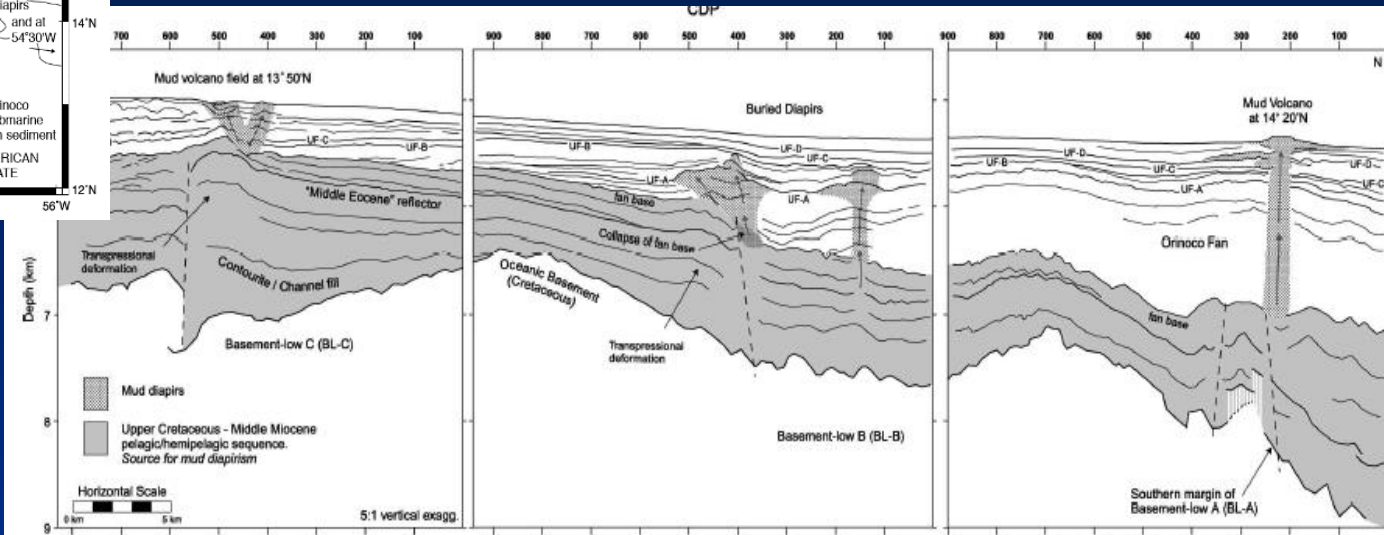
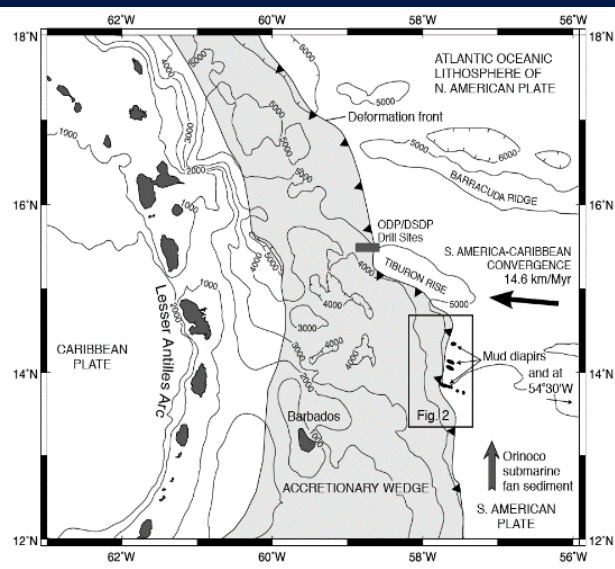
Da Deville et al. 2007



Da Deville, 2009

Figure 2. Field of mud volcanoes in the eastern continental slope of the offshore of Trinidad.

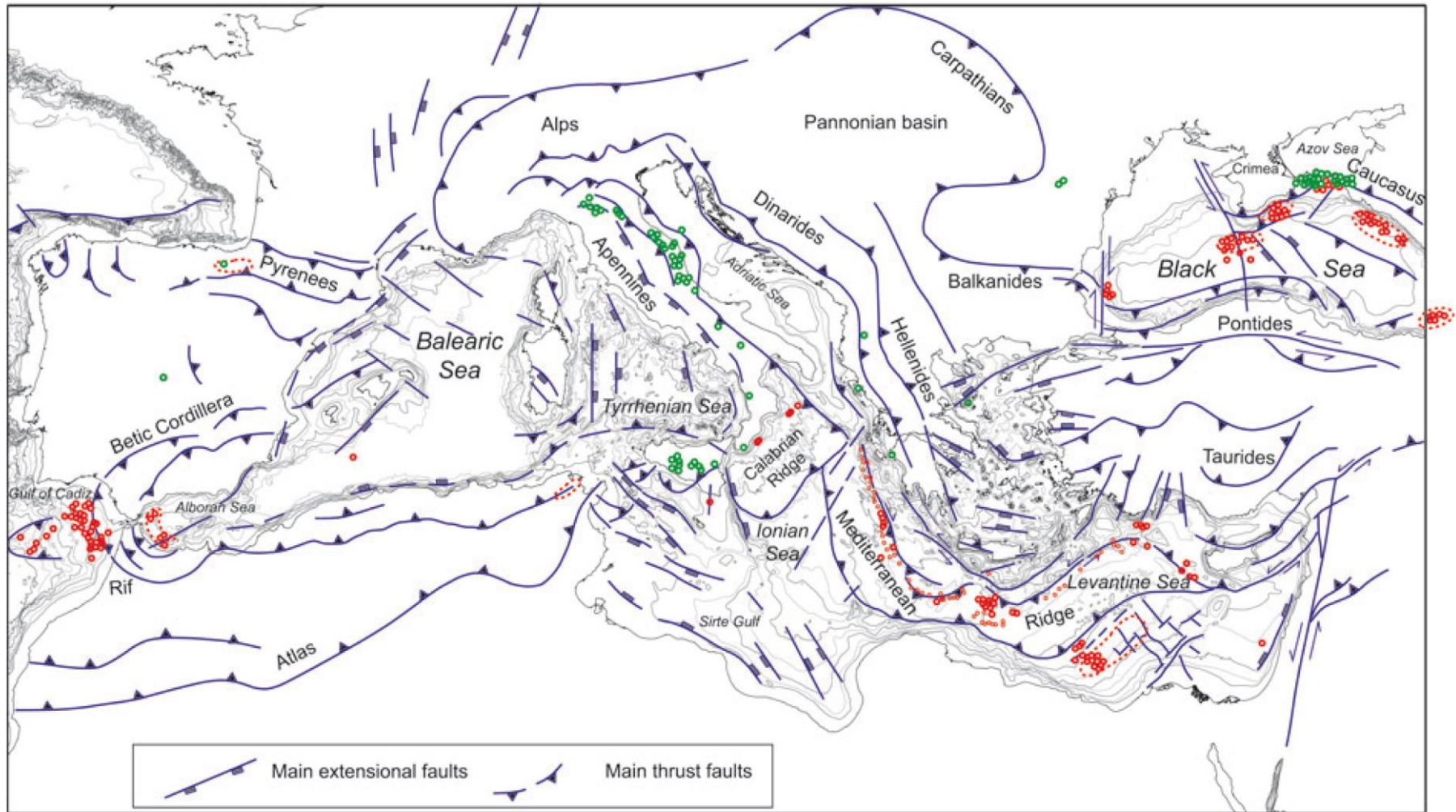
Diapiri di fango in avanfossa, Barbados



Sumner & Westbrook, 2001. *Marine and Petroleum Geology*, 18, 591-613.

Diapiri e vulcani di fango

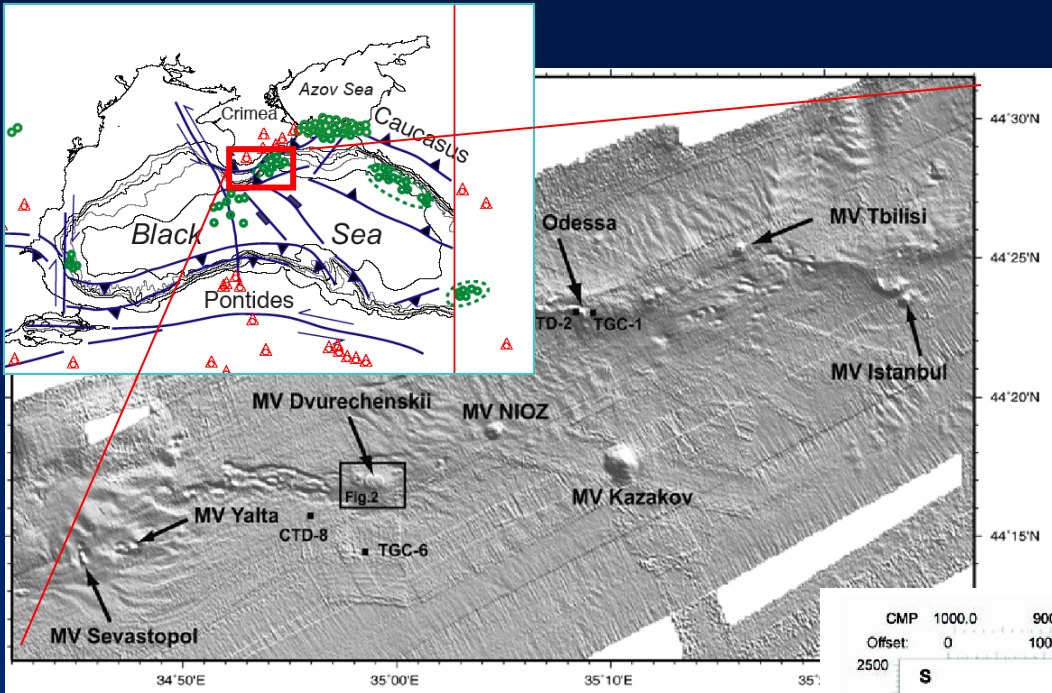
MUD VOLCANOES IN THE MEDITERRANEAN REGION



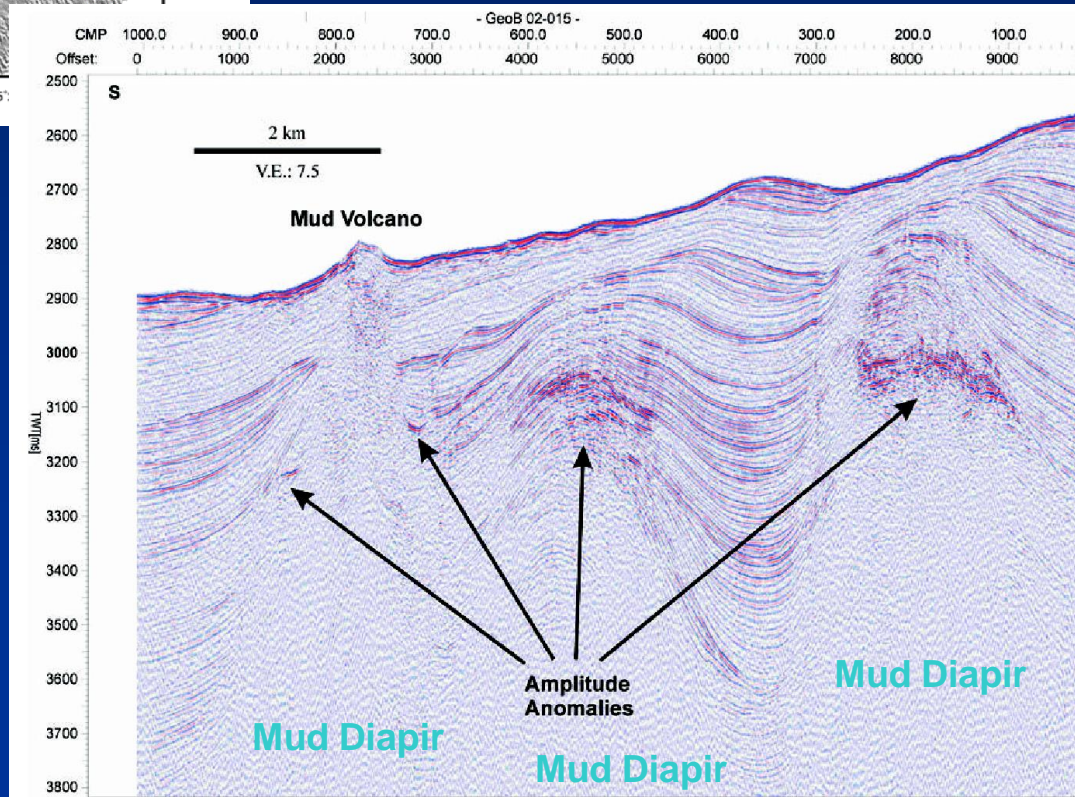
Da Camerlenghi & Pini, 2009

BLACK SEA MUD VOLCANOES

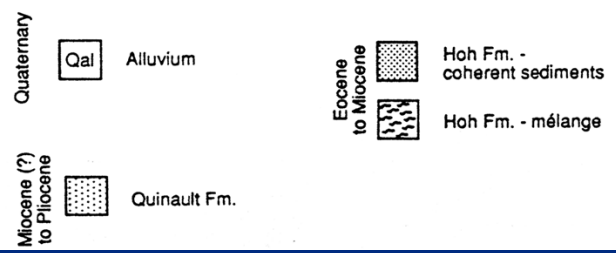
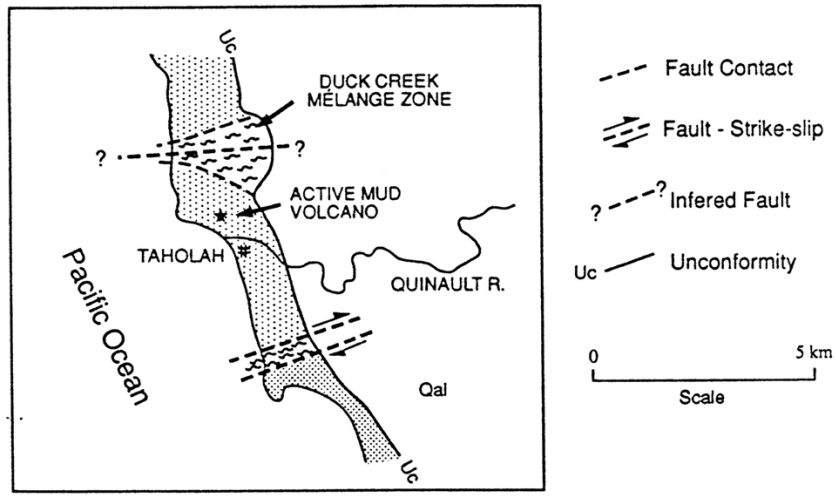
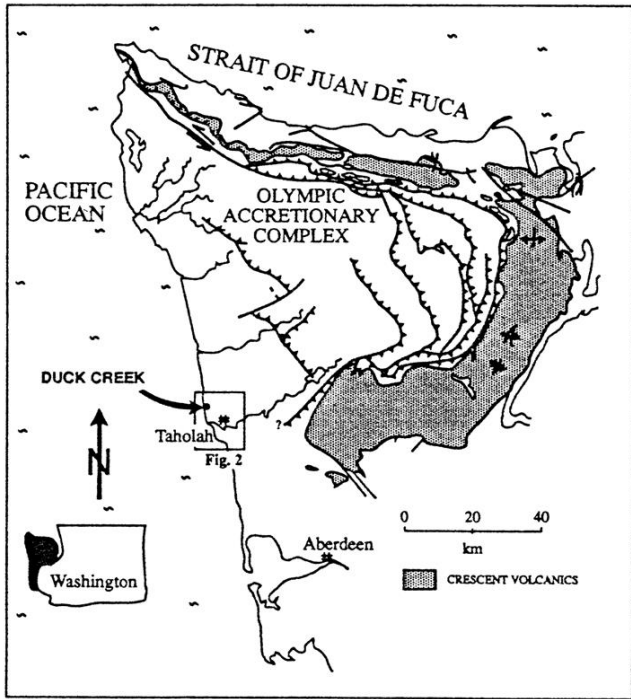
Da Krastel et al., 2003



Da Bohrmann et al., 2003



Courtesy of A. Camerlenghi



Brown & Orange, 1993

Fig. 1. Location of the Olympic Peninsula, Washington, U.S.A. The Duck Creek mélangé is located on the coast of the Peninsula approximately 10 km north of Taholah, near the southern limit of the exposed Olympic accretionary complex (after Tabor & Cady 1978, Snavley & Kvenvolden 1988).

Duck Creek mélangé: un diapiri di fango

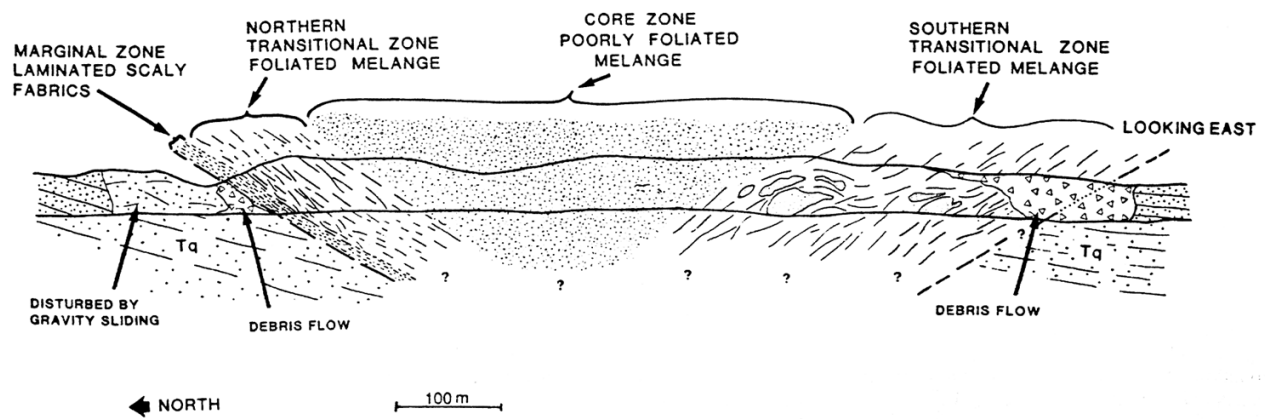


Fig. 4. Cross-section through the Duck Creek mélangé, view is to the east. With the exception of the slumped contacts, the mélangé has near 100% exposure along the steep 20 m sea cliffs. These steep exposures have the advantage of corresponding to a cross-section of the mélangé.

GAPini



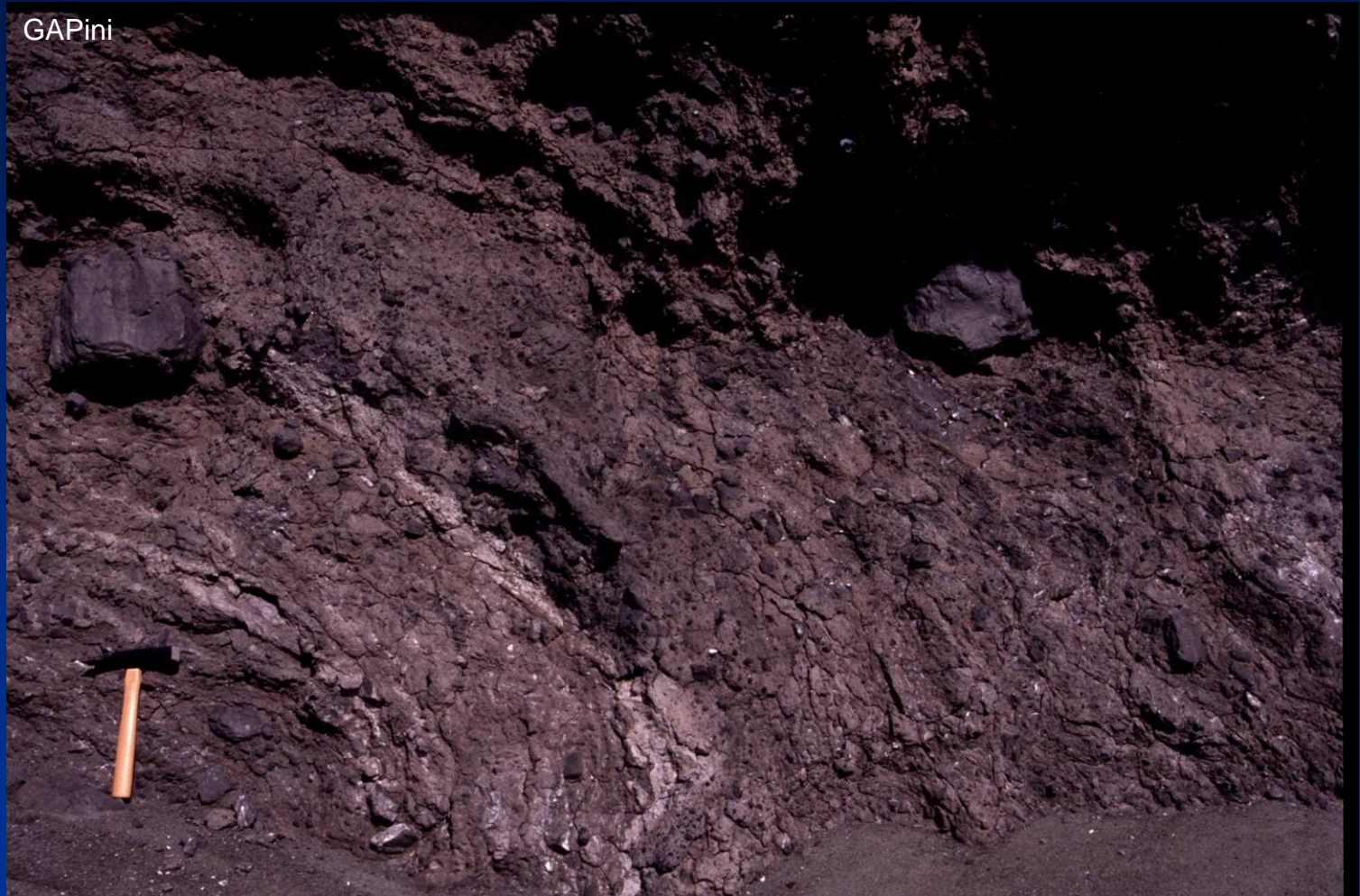
GAPini



GAPint



GAPini



GAPini

